https://doi.org/10.5194/egusphere-2023-2581
Preprint. Discussion started: 9 November 2023

Coccolithophorids precipitate carbonate in clumped isotope equilibrium with seawater

Alexander J. Clark[1], Ismael Torres-Romero[1], Madalina Jaggi[1], Stefano M. Bernasconi[1], and Heather M. Stoll[1]

[1]Department of Earth Sciences, ETH Zürich, Switzerland

Correspondence to: Alexander J. Clark (aclark@ethz.ch)

Abstract. Numerous recent studies have tested the clumped isotope (Δ_{47}) thermometer on a variety of biogenic carbonates such as foraminifera and bivalves and showed that all follow a common calibration. While the sample size requirements for a reliable Δ_{47} measurement have decreased over the years, the availability and preservation of many biogenic carbonates is still limited and/or require substantial time to be extracted from sediments in sufficient amounts. We thus determined the Δ_{47}-temperature relationship for coccolith carbonate, which is abundant and often well-preserved in sediments. The carbon and oxygen isotopic compositions of coccolith calcite have limited use in palaeoenvironmental reconstructions due to physiological effects that cause variability in the carbon and oxygen isotopic values. However, the relatively limited data available suggest that clumped isotopes may not be influenced by these effects. We cultured three species of coccolithophores in well-constrained carbonate system conditions with a $CO_{2(aq)}$ between 5 and 45 µM and temperatures between 6°C and 27°C. Our results agree with a previous culture study that there are no species- or genus-specific effects on the Δ_{47}-temperature relationship in coccolithophores and find that varying environmental parameters other than temperature also do not have a significant effect. Our coccolith-specific Δ_{47}-temperature calibration agrees within ±1°C of other biogenic carbonate calibrations yet all biogenic carbonate calibrations show a consistent offset of ≥2°C relative to the inorganic carbonate calibrations. Thus, all biogenic specific calibrations can be used interchangeably and must be used for the reconstruction of calcification temperatures in biogenic carbonates.

1 Introduction

Clumped isotope thermometry is a relatively new and increasingly used methodology for the reconstruction of paleotemperatures, palaeohydrology, diagenetic regimes, and as an isotopic tracer (see Huntington and Petersen, 2023 for a recent review). In a carbonate molecule, bonds between the rare isotopes ^{13}C and ^{18}O are thermodynamically preferred, leading to an increase in their abundance – denominated as "clumping" – with decreasing temperature. To measure this clumping, the carbonate is converted to CO_2 by reaction with phosphoric acid, and the excess abundance of ^{13}C and ^{18}O atoms (cardinal mass 47) in the released CO_2 relative to stochastic distribution is measured and reported as Δ_{47} (Schauble et al., 2006; Eiler, 2007). In early studies, before the introduction of carbonate standardisation (Bernasconi et al. 2021), Δ_{47} in different calibration

https://doi.org/10.5194/egusphere-2023-2581
Preprint. Discussion started: 9 November 2023

studies had widely variable relationships with temperature. However, more recent studies have shown that these discrepancies were caused by poor interlaboratory comparability (Bernasconi et al. 2018, 2021; Anderson et al. 2021).

Based on these recent studies, Δ_{47} has a consistent relationship with temperature, independent from the origin of the carbonate, and its temperature dependence is well established empirically at a large range of temperatures (e.g., Anderson et al., 2021; Fiebig et al., 2021). The Δ_{47}-temperature relationship is independent of the carbon and oxygen isotope composition of the fluid from which carbonates precipitate (Ghosh et al., 2006). Empirical calibrations between temperature and Δ_{47} have been established for temperatures between 0°C and 1100°C for inorganic carbonates (Kele et al., 2015; Bonifacie et al., 2017; Kelson et al., 2017; Müller et al., 2019; Anderson et al., 2021). Further empirical studies on biogenic carbonates, such as for foraminifera, coccoliths, gastropods, and bivalves, have found similar relationships between Δ_{47} and calcification temperature (Katz et al., 2017; Peral et al., 2018; Leutert et al., 2019; Piasecki et al., 2019; de Winter et al., 2022; Huyghe et al., 2022). Apart from specific types of biogenic carbonates such as shallow-water corals (Spooner et al., 2016), juvenile bivalves (Huyghe et al., 2022), and brachiopods (Letulle et al., 2023), these biogenic calibrations all fall within the same confidence interval (Meinicke et al., 2020, Jautzy et al. 2020, Anderson et al. 2021; Daëron and Gray, 2023).

While most calibrations are consistent for inorganic and biogenic calcite, other methodological problems limit the overall use of clumped isotopes. The relative abundance of Δ_{47} to all isotopologues of CO_2 is only ~45 ppm, which requires a sample in the range of 80 to 120 µg with Thermo-Fischer Kiel IV devices coupled to Thermo-Fischer 253 Plus mass spectrometers (Müller et al., 2017) to 2-10 mg for a single measurement with common acid bath systems (e.g. Ghosh et al., 2006; Kelson et al., 2017; Peral et al., 2018; Fiebig et al., 2021). As the analytical error in clumped isotope measurements is large compared to the natural variability, many replicates are needed to achieve an analytical uncertainty allowing meaningful interpretations in palaeoceanography (Bernasconi et al., 2021; Fernandez et al., 2017; Daëron, 2021). Sample size requirements are a major limiting factor for biogenic calcite with limited sample availability such as foraminifera from cores and core-tops or slow-growing molluscs (Leutert et al., 2019; de Winter et al., 2022; Huyghe et al., 2022). Coccoliths are a promising alternative as they are often found in greater abundance and have a better preservation potential than foraminifera (Berger, 1973; Subhas et al., 2019). The abundance of coccolith-associated-polysaccharides (CAP) both around and within the coccolith aid in protecting the coccolith calcite from dissolution and overgrowth, and remain in place for millions of years (Henriksen et al., 2004; Sand et al., 2014; Lee et al., 2016). Few anion substitutions and a lack of lattice defects on the coccolith surface further aid in a better preservation relative to foraminifera (Berman et al., 1993; Stoll et al., 2001; Frøhlich et al., 2015; Walker et al., 2019).

Kinetic and disequilibrium effects due to the biological origin of the calcite, collectively known as vital effects, are known to affect the carbon and oxygen isotopic composition of coccolith calcite (Ziveri et al., 2003; Rickaby et al., 2010; Ziveri et al., 2012; Candelier et al., 2013; Hermoso et al., 2014; Stevenson et al., 2014; Hermoso et al., 2016, Katz et al., 2017). Initial studies find that multiple coccolithophore species with different carbon and oxygen vital effects do follow previous Δ_{47}-temperature calibrations (Drury and John, 2016; Katz et al., 2017). However, these calibrations were performed before carbonate standardisation (Bernasconi et al., 2021) and have a limited number of replicate analyses, limiting their robustness

https://doi.org/10.5194/egusphere-2023-2581
Preprint. Discussion started: 9 November 2023

and interpretation. Other aspects such as the dissolved inorganic carbon chemistry in the cultures and growth conditions as possible influences on Δ_{47} also still need to be examined.

To this end, three species of calcifying coccolithophores were cultured under controlled temperature and carbonate chemistry conditions. A temperature range of 21°C and $CO_{2(aq)}$ range of 40 µM was covered. Coccolithophores from the *Gephyrocapsa* genus were cultured between 6°C and 27°C, using the warm-adapted *G. oceanica* and the cold-adapted *G. muellerae*. Inter-genus vital effects were tested through comparison with *Calcidiscus leptoporus*. Finally, through comparison with a previous coccolith culture (Katz et al., 2017), inorganic (Anderson et al., 2021), biogenic (Peral et al., 2018; Meinicke et al., 2020; de Winter et al., 2022), and recalculated (Daëron and Gray, 2023) Δ_{47}-temperature calibrations, the potential need for a coccolith-specific calibration is assessed.

2 Materials and methods

2.1 Batch and continuous culture setup

Three monoclonal coccolithophore strains, *Gephyrocapsa oceanica* (RCC 1303), *Gephyrocapsa muellerae* (RCC 3370), and *Calcidiscus leptoporus* (RCC 1130) obtained from the Roscoff Culture Collection were cultured at ETH Zürich. *G. oceanica* is an abundant cosmopolitan coccolithophore species that has been found at temperatures between 12-27°C but favours temperatures above 20°C (Sett et al., 2014; von Dassow et al., 2021). *G. muellerae* is from the same genus as *G. oceanica*, favours colder and less saline conditions, and can grow at 6°C (von Dassow et al., 2021). *C. leptoporus* is a large coccolithophore, is especially abundant in low latitude upwelling settings, is resistant to dissolution and thus a major contributor to coccolith carbonate, and is known to have large isotopic vital effects (Thierstein and Young, 2004; Ziveri et al., 2007; Langer et al., 2012; Hermoso, 2014). Thus, the three strains were cultured to provide a temperature range of 21°C while also highlighting potential isotopic vital effects. *G. oceanica* was cultured in a turbidostat or continuous culture setup as seen in Fig. 1a, between a $CO_{2(aq)}$ of 5 and 45 µM for at least two temperatures (Table 1). All three strains were grown in at least two temperatures in batch culture setup as seen in Fig. 1b, and provide a wide range of temperatures (Table 1).

All cultures were carried out in Artificial Seawater (ASW), following Kester et al. (1967), as the basis of a K/2 medium (Keller et al., 1987). The final pH and DIC were adjusted through addition of HCl and Na_2CO_3 and covered a range of 40 µM of $CO_{2(aq)}$ values. A Tris buffer was not included for all experiments as this would interfere with the carbonate chemistry control. Prior to inoculation, the K/2 media was sterilized through an 0.2 µm Millipore Stericup filter.

Before starting the experiments, the strains were maintained at a constant temperature of 18°C and slowly acclimatized to the experimental temperature for at least 4-6 generations. Cultures were inoculated at cell densities of ~5000 cells mL^{-1} for *G. oceanica* and *G. muellerae* and ~2000 cells mL^{-1} for *C. leptoporus*.

Batch cultures were carried out in 1 or 2 L Nalgene polycarbonate sterile flasks with 50- and 100-mL headspace respectively and kept in a lit incubator set to the experimental temperature (± 0.1°C). For the duration of the experiments, the flasks were

https://doi.org/10.5194/egusphere-2023-2581
Preprint. Discussion started: 9 November 2023

rotated on a roller set at 10 rpm to reduce settling and allow for uniform light exposure, see Fig. 1b. *C. leptoporus* did not grow under turbulent conditions and was manually shaken every day (Houdan et al., 2006). The cultures were illuminated by LED lights on a sinusoidal 14/10-hour light/dark cycle and a maximum luminosity of 120 µmol photons m^{-2} s^{-1}. Harvesting took place in a semi-continuous manner, where 80-90% of the total volume was harvested and then refreshed when the culture reached a set cell density (100-150 x 10^3 cells mL^{-1}). In general, we used a higher cell density compared to previous culturing studies due to the larger sample material requirement for clumped isotope measurements. Yet each strain was maintained in their early- to mid-exponential phase to prevent a reservoir effect and an enriching of the $\delta^{13}C$ of the media ($\delta^{13}C_{DIC}$) relative to the initial conditions (Barry et al., 2012; Hermoso, 2014). Certain batch and continuous cultures had a higher cell density and significant drift in the DIC, pH, or $CO_{2(aq)}$ over the course of the experiment and serve to test the sensitivity of vital effects to a varying carbon system.

Continuous cultures were performed in 1L (FMT 150/1000) or 3L (FMT 150/3000) photobioreactor (PBR) connected to a PP600 peristaltic pump and a GMS 150 gas mixing system (Photon Systems Instruments, Drásov, Czech Republic), see Fig. 1a. For a more detailed description of the experimental setup see Zhang et al. (2022). The strains were illuminated with LEDs on a 16/8-hour light/dark cycle with a maximum luminosity of 200 µmol photons $m^{-2}s^{1}$. The optical density (OD), which is proportional to the cell density, was calibrated to a zero point before inoculation. With continuous OD monitoring and (sub-)daily measurements of the cell density, the OD could be set to a cell density threshold between 100 and 200 x 10^3 cells mL^{-1}. If the OD exceeded this threshold, the peristaltic pump pumped fresh media into the PBR equivalent to 10% of the culture volume, and media from inside the PBR was pushed into the outflow bottle. Ambient air was first scrubbed of CO_2 and then passed through a gas mixing system with a set amount of CO_2 with a constant composition ($\delta^{13}C$ = -14.36 ± 0.06‰ VPDB; $\delta^{18}O$ = 19.85 ± 0.14‰ VSMOW). Thus, the pCO_2 was controlled and maintained at a constant level, which was checked at the beginning and end of each experiment. Temperatures were continuously controlled with a pH-temperature probe in the vessel, which kept a constant temperature with <0.1°C deviation through Peltier-elements at the bottom of the vessel.

Cell density and size were measured using a Z2 Coulter Particle Counter and Size Analyzer with an aperture size of 100 µm (Beckman Coulter, Inc., Brea, California, United States), which were used to determine growth rates. Cell counts were taken systematically every 24 hours with an extra measurement taken before and after harvest.

The net growth rate for batch cultures were calculated as:

$$\mu = \frac{\ln(N_t) - \ln(N_0)}{t - t_0} \quad (1)$$

where N_t is the cell count at time t (in days) and N_0 is the initial cell count.

For continuous cultures, the dilution rate, which equates to the volume of the output (V_{out}) over the volume of the PBR over time t also needs to be considered:

$$\mu = \frac{\ln(N_t) - \ln(N_0) + \frac{V_{out}}{V_{PBR}}}{t - t_0} \quad (2)$$

https://doi.org/10.5194/egusphere-2023-2581
Preprint. Discussion started: 9 November 2023

Cells were harvested by centrifugation at 4000 rpm for 5 minutes. The pellet containing coccoliths was rinsed with deionized water to remove traces of salts by 4 cycles of centrifugation and removal of the supernatant. Subsequently, the wet pellet of organic matter and coccoliths was transferred to a 2 mL vial, which was then stored at -20°C for later analysis.

At the beginning, at each harvest, and at the end of an experiment, 12 mL of water were sampled for pH and cell density measurement. Each aliquot was centrifuged once at 4000 rpm for 5 minutes, and the supernatant was used for DIC, $\delta^{13}C_{DIC}$, and $\delta^{18}O_{SW}$ measurements. Some batch and continuous cultures were kept until higher cell densities were reached. In these cases, pH, DIC, and $\delta^{13}C_{DIC}$ were measured more often to track the evolutions from initial conditions as a result of cell growth and cell density increase.

2.2 Sample cleaning

Contaminants from organic matter or sulphur compounds contained within carbonates are known to interfere with the clumped isotopic measurements for carbonates (Eiler and Schauble, 2004; Dennis and Schrag, 2010). In this study we used three methodologies for the removal of possible contaminants from the coccolith pellet. Initially the aliquots were dried in a 60°C oven for at least 4 hours to remove any remaining water that could dilute the cleaning reagents. Then one of three cleaning methodologies was performed.

One method used oxidation of the organic matter through reaction with a 18% H_2O_2 solution neutralized with NaOH to pH 8-9 following the protocol of Falster et al. (2018). The second methodology used a solution of 10% H_2O_2 neutralized with NH_3 to pH 8-9. For both solutions the pellets were reacted overnight at room temperature and then rinsed 4-5 times with milli-Q until a neutral pH of 7 was obtained. The third method used is Total Lipid Extraction (TLE), following Matyash et al. (2008). The pellets were first reacted with 1 mL of isopropanol and homogenized through vortexing and sonication until there were no visible clumps. 3 mL of methyl-tert-butyl ether (MTBE) were added and the total solution was again vortexed. 1 mL of DI water was added and the sample was centrifuged at 4000 rpm for 5 minutes. This method removes the polar and apolar organic compounds from the pellet into the upper 4 mL of the solution. This supernatant is subsequently discarded, while maintaining a 1 mL of aqueous phase with the cleaned coccolith pellet at the bottom. When abundant organic matter was still visible after one cycle of cleaning, the procedure was repeated. After all three cleaning methodologies, the samples were dried at 60°C for at least 4 hours.

In order to confirm the effectiveness of the different cleaning methodologies and their effect on the coccolith carbonate, high resolution scanning electron images were taken using a JSM-7100F JEOL Scanning electron Microscope (SEM) at ScopeM, ETH Zürich, see Fig. S1.

https://doi.org/10.5194/egusphere-2023-2581
Preprint. Discussion started: 9 November 2023

2.3 Isotope measurements

2.3.1 Coccolith carbon, oxygen, and clumped isotopes

Carbon, oxygen, and clumped isotopes from the cultured coccoliths were measured on two ThermoFisher Scientific mass spectrometers, a MAT253 and a 253Plus, coupled to Kiel IV preparation devices as described in Müller et al. (2017). Aliquots of 110-180 µg of sample and carbonate standards (ETH-1, 2, 3, and IAEA C2) were measured with a Kiel device at 70°C. The samples were reacted for 300 seconds with three drops of 104% phosphoric acid, and the released CO_2 was immediately frozen in a liquid nitrogen (LN_2) trap kept at -190°C. After the sample was reacted fully, the first LN_2 trap is heated to -100°C, and the CO_2 gas was transferred through a 10 mm PorapakQ (50-80 mesh) to a second LN_2 trap kept at -190°C. The PorapakQ tubing was coated with Sulfinert 2000, stuffed with silver wool, and kept at -40°C to capture and eliminate possible organic contaminants. The second LN_2 trap was then heated to room temperature and measured using the Long Integration Dual Inlet (LIDI) protocol (Hu et al., 2014, Müller et al., 2017). The initial gas intensity of the sample gas is recorded and then immediately measured for 400 seconds, 40 cycles of 10 seconds. Subsequently, the reference gas is measured for the same duration starting at the same initial gas intensity. Before measuring, background scans at different beam intensities were carried out to determine the pressure dependent background on all beams (Bernasconi et al., 2013; Meckler et al., 2014). Using the Easotope software (John and Bowen, 2016) a pressure-sensitive baseline (PBL) correction was applied, and raw carbon and oxygen values were converted to VPDB using the Brand parameters as suggested by Daëron et al. (2016). Further, the raw vs accepted Δ_{47} values for the carbonate standards and an empirical transfer function (ETF) were used to convert and normalize the sample Δ_{47} data to the Intercarb carbon dioxide equilibrium scale (I-CDES; Bernasconi et al., 2021).

Each individual reported clumped isotope value consists of at least 10 replicates. Long-term accuracy and reproducibility of the Δ_{47} measurements were evaluated based on monitoring of the IAEA-C2 international carbonate standard (MAT253: Δ_{47} = 0.6385 ± 0.034, MAT253 Plus: Δ_{47} = 0.6411 ± 0.026‰; 1σ) and fit within the accepted values (0.6409‰ ± 0.003‰; Bernasconi et al., 2021). Analytical errors are reported at the 95% confidence interval (Fernandez et al., 2017).

2.3.2 DIC and seawater carbon and oxygen isotopes

DIC and pCO_2 were measured on a Picarro G-2131-i Cavity Ringdown Spectrometer (CRDS; Picarro Inc, USA) coupled to a AS-D1 DIC-$\delta^{13}C$ Analyzer (Apollo Scitech, USA). For DIC measurements, 3 mL of centrifuged media were taken and reacted within the AS-D1 analyser with 0.9 mL of a 3% H_2PO_4 and 7% NaCl solution. The absolute DIC concentration was found through quantification of the extracted CO_2 concentration as described in Deng et al. (2022). A threshold of ≤20 ppm pCO_2 for background synthetic air (80% N_2, 20% O_2; PanGas) was first defined. After at least 10 measurements of background air below this threshold, the stable baseline was reached and the sample is injected into the measuring chamber. As the extracted CO_2 flows into the measuring chamber, measurements of pCO_2 were taken every 3-5 seconds until all of the extracted CO_2 had passed through the measuring chamber, and the stable baseline was reached again. For the absolute DIC concentration, the integrated area of pCO_2 between the two baselines is plotted against the total DIC content. The latter is defined as the

https://doi.org/10.5194/egusphere-2023-2581
Preprint. Discussion started: 9 November 2023

volume multiplied by the measured DIC. A Certified Reference Material (CRM), NOAA batch 186 with a known absolute DIC concentration of 2012 µM, is used for calibration. Through variation of the CRM volume, a range of integration areas and total DIC content was obtained and internally defined. Two secondary standards with calibrated DIC concentrations were also used. Each measurement was repeated twice with the same centrifuged media in quick succession to reduce CO_2 exchange with the atmosphere, which gave an average DIC and uncertainty for each measured sample.

For $\delta^{13}C_{DIC}$ measurements, 1 mL of centrifuged media was acidified with 150µL of 104% H_2PO_4 in a He-flushed vial. Subsequently the $\delta^{13}C_{DIC}$ was measured on a Gasbench II coupled to a Delta V Plus mass spectrometer (Thermo Fischer Scientific, USA). Two in-house $NaHCO_3$ standards dissolved in deionized water with $\delta^{13}C_{DIC}$ values of -4.66‰ and -7.94‰ were used.

The oxygen isotopic composition of the seawater ($\delta^{18}O_{sw}$) was measured on a Picarro L2130-*i* Isotope Wavelength-Scanned Cavity Ring-Down Spectrometer (WS-CRDS) following Gupta et al. (2009). The water sample is first passed through a salt catchment trap, vaporized, and injected at a uniform concentration and flow rate into the WS-CRDS. This delivers a pulse with a constant concentration profile, during which the $\delta^{2}D$ and $\delta^{18}O$ are measured. Three in-house standards calibrated to three IAEA and USGS standards (SLAP2, GRESP, and VSMOW2) were run every 20 samples. Another in-house standard is run as an unknown sample. All standards fell within 1 standard deviation of their accepted value. Measurement precision was affected by the residual salt from the seawater. At least two seawater measurements were taken for each experiment. Subsequently an average $\delta^{18}O_{sw}$ and uncertainty for each condition was obtained, see Table S1. This uncertainty is used for the uncertainty of the oxygen isotope offset from seawater, $\delta^{18}O_c - \delta^{18}O_{sw}$ ($\Delta^{18}O_{c\text{-}sw}$) as reported in Table 1, and will be used in subsequent figures.

pH measurements were made using a Mettler Toledo LE410 pH-probe (Mettler Toledo, Greifensee, Switzerland) and were calibrated with three NBS standards (pH=4.00, 7.01, 9.03 at 21°C), with a standard deviation of ±0.01. All pH measurements are given in the NBS scale. Seawater carbon chemistry was calculated through CO2SYS (Lewis and Wallace, 1998), with input of measured pH and DIC, and using the K1, K2 constants of Leuker et al. (2000), $KHSO_4$ of Dickson (1990), KHF of Perez and Fraga (1987), and $[B]_I$ value of Lee et al. (2010).

DIC and pH measurements are compared and normalized to the initial measured values to detect potential drift and stability of the carbon chemistry of each culture. These are reported as initial DIC – measured DIC (Δ_{DIC}) and initial pH – measured pH (Δ_{pH}) in Table S1. We report the uncertainty of the fractionation between coccolith calcite and DIC ($\Delta^{13}C_{c\text{-}DIC}$) as the standard deviation of all measured $\delta^{13}C_{DIC}$ over the course of the sampled culture, to take into account the potential effect of DIC evolution and drift, and will be used in subsequent figures.

The same media was used for both batch and continuous cultures and thus the same $\delta^{13}C_{DIC}$ would be expected for both. However, through the continuous bubbling and gas-exchange in the continuous cultures, there is a potential for different $\delta^{13}C_{DIC}$ values than the batch culture setup. Indeed, there is a non-systematic enrichment of 0-1‰ for the batch culture $\delta^{13}C_{DIC}$. However, the fractionation between coccolith calcite and DIC i.e. $\Delta^{13}C_{c\text{-}DIC}$, is not affected by these differences.

https://doi.org/10.5194/egusphere-2023-2581
Preprint. Discussion started: 9 November 2023

An often-used index in coccolithophore geochemistry studies (McClelland et al., 2017; Phelps et al., 2021) for the relative usage of carbon supply and demand is the dimensionless τ:

$$\tau = \frac{r*\rho*\mu}{3*CO_{2(aq)}*P_c} \quad (3)$$

It reflects the degree of carbon utilization by the coccolithophore as measured through growth rate (μ), defined in Eqs. 1 and 2 for batch and continuous culture setup respectively, the cell radius (r), and cellular carbon density (ρ) against the DIC supply into the cell ($CO_{2(aq)}$) and the permeability to CO_2 (P_c). We use a P_c of 1.4 x 10^{-3} μm day^{-1} (Blanco-Ameijeiras et al., 2020) and ρ of 2 x 10^{-3} μM (McClelland et al., 2017). It is assumed that there is only a diffusive supply of CO_2 into the cell. Our cell size measurements assume a perfect coccosphere for each counted cell, which results in a coccosphere radius that is slightly different than the cell radius. This is taken into account, together with uncertainties in μ and $CO_{2(aq)}$, into the uncertainty of the final τ value.

3 Results

3.1 Carbon chemistry

3.1.1 DIC, pH, and $CO_{2(aq)}$

The stability of the carbon chemistry was monitored with at least three DIC and pH measurements for each culture. Drift from the initial conditions was less than ±20% and ±0.20 for Δ_{DIC} and Δ_{pH} respectively for 40 culture experiments (Fig. S2 and Table S1). To ensure only well-constrained culture conditions are considered, fifteen experiments with $\Delta_{DIC} \geq 20\%$ or $\Delta_{pH} \geq 0.20$ are excluded from our main analysis in Figs. 2 through 5, but are evaluated in a subsequent comparison (see Sect. 4.3).

3.1.2 Carbon isotopes

The carbon isotope composition of the DIC ($\delta^{13}C_{DIC}$) varies between -5.10‰ and 0.80‰, with a similar large range of -5.52‰ and -0.07‰ for all species' coccolith carbon isotopes ($\delta^{13}C_c$; Table S1). This is mostly due to the large variability in $\delta^{13}C_c$ for *G. oceanica*, which can be attributed to the range of different experimental conditions. The $\delta^{13}C_c$ in *G. muellerae* varies between -4.68‰ and -3.66‰, while the $\delta^{13}C_c$ in *C. leptoporus* varies between -5.15‰ and -5.04‰.

The fractionation $\Delta^{13}C_{c\text{-}DIC}$, ranges between -1.41‰ and 1.22‰ for *G. oceanica*, -0.88‰ and 0.21‰ for *G. muellerae* and -2.86‰ and -2.22‰ for *C. leptoporus*. Pearson correlation coefficients (ρ) are used to determine whether two parameters are linearly correlated. If the ρ value is near 1 or -1, there is a strong correlation and one parameter has an effect on the other. Weak correlations are here defined as $\rho \leq \pm 0.40$ and significance is given by a p-value < 0.05. No significant linear correlations were identified between *Gephyrocapsa* $\Delta^{13}C_{c\text{-}DIC}$ and carbonate system parameters (DIC, pH, $CO_{2(aq)}$) or culture parameters (cell density and Δ_{DIC}) (Table S2). *Gephyrocapsa* culture data is also not significantly correlated with τ, the index of carbon demand vs supply (Fig. 2; ρ = 0.06, p-value = 0.74). Including *Calcidiscus* does not improve the correlation or significance with any parameter apart from Δ_{DIC}.

https://doi.org/10.5194/egusphere-2023-2581
Preprint. Discussion started: 9 November 2023

3.2 Oxygen isotopes

The $\delta^{18}O_{sw}$ are given in Table S1 for all cultures and vary by ~1.6‰ across with no systematic differences between batch and continuous cultures. For a given temperature, *C. leptoporus* has systematically lower $\delta^{18}O_c$ values by ~3‰ while *G. oceanica* and *G. muellerae* have similar $\delta^{18}O_c$ values at the same temperature. The interspecies variations are independent of culture setup and experimental condition.

The oxygen isotope offset from seawater, $\delta^{18}O_c - \delta^{18}O_{sw}$ ($\Delta^{18}O_{c\text{-}sw}$), varies systematically for all experimental conditions as seen in Fig. 3 and Table 1. *Calcidiscus* has a systematic offset of ~3‰ relative to *Gephyrocapsa* at the cultured growth temperatures, which agrees with previous culturing studies (Ziveri et al., 2003; Candelier et al., 2013; Stevenson et al., 2014; Hermoso et al., 2016; Katz et al., 2017). For *G. oceanica*, there is a significant negative correlation between $\Delta^{18}O_{c\text{-}sw}$ and temperature (ρ = -0.94, p-value <0.05), which remains when including *G. muellerae* (ρ = -0.97, p-value <0.05). The $\Delta^{18}O_{c\text{-}sw}$-temperature relationship is consistent between setups and experimental conditions and is not influenced by the variability in $\delta^{18}O_{sw}$ values. The $\Delta^{18}O_{c\text{-}sw}$ is thus genus- but not species-specific.

3.3 Clumped isotopes

The Δ_{47} values are shown in Table 1 and Fig. 4, and range from 0.589‰ – 0.640‰ for temperatures between 12-27°C for *G. oceanica*, 0.618‰ – 0.659‰ between 6-18°C for *G. muellerae*, and 0.636‰ – 0.652‰ at 12°C for *C. leptoporus*. There is variation of ~25 ppm at given experimental conditions, in particular at 21°C and 24°C, although all datapoints fall within the long-term standard deviation of the standards used for correction of 0.020‰. There is no difference between species or genus at given temperatures.

4 Discussion

Disequilibrium in the carbon, oxygen, and clumped isotopic systems is driven by different mechanisms within the DIC-H_2O system and coccolithophore cells. Thus, in order to fully evaluate potential vital effects in the Δ_{47}-temperature relationship in coccolith calcite, we first characterize and discuss the vital effects in carbon and oxygen isotopes and compare them to previous culture studies.

4.1 Carbon isotope vital effects in coccolith calcite

In this study (Fig. 5), all continuous (and most batch) cultures for *G. oceanica* fall within the expected range of 0 ± 1.5‰ for $\Delta^{13}C_{c\text{-}DIC}$ as found in other studies (see Fig. S3; Rickaby et al., 2010; Moolna and Rickaby, 2012; Hermoso, 2014; Katz et al., 2017). There are no comparable culture studies for *G. muellerae*. The $\Delta^{13}C_{c\text{-}DIC}$ values fall within the range of *G. oceanica*. Both species will be combined in any inter-genera analyses for Sect. 4. *C. leptoporus* has a $\Delta^{13}C_{c\text{-}DIC}$ of -2.0 ± 1.0‰ comparable to previous culturing studies (Fig. 5; Ziveri et al., 2003; Hermoso et al., 2014; Katz et al., 2017).

https://doi.org/10.5194/egusphere-2023-2581
Preprint. Discussion started: 9 November 2023

Models of the vital effect in coccolith carbon universally consider two fundamental controls on $\Delta^{13}C_{c\text{-}DIC}$ (Bolton and Stoll, 2013; Holtz et al., 2017; McClelland et al., 2017). For a given cell size and growth rate, all available models simulate a decrease in $\Delta^{13}C_{c\text{-}DIC}$ with increasing concentrations of $CO_{2(aq)}$. An increase in $CO_{2(aq)}$ relative to the cellular carbon demand will result in a decrease in $\Delta^{13}C_{c\text{-}DIC}$. The carbon supply versus demand index τ is often used to describe this behaviour (Eq. 3, Fig. 2). However, we cannot discern whether our *Gephyrocapsa* experiments show such a decrease in $\Delta^{13}C_{c\text{-}DIC}$. One contributing factor may be the positive correlation of $CO_{2(aq)}$ with DIC in our experiments, due to our strategy of manipulating the carbon system through bubbling CO_2 into the system. Previous models simulate an increase in $\Delta^{13}C_{c\text{-}DIC}$ when there is an increase in the proportion of HCO_3^- relative to CO_2 entering the cell as the greater proportion of HCO_3^- will cause an enrichment in the $\delta^{13}C$ of the intracellular reservoir. Although carbon limitation at low $CO_{2(aq)}$ levels is observed to increase HCO_3^- uptake into the cell (Rost et al., 2003; Bach et al., 2013), it is also possible that higher media DIC can also lead to an increased HCO_3^- uptake and compensate the expected effect of higher $CO_{2(aq)}$. Interspecific variations in $\Delta^{13}C_{c\text{-}DIC}$ are strongly conditioned by the PIC:POC ratio. The high PIC:POC ratio of *Calcidiscus* contributes to a lowering of the $\delta^{13}C_c$ and $\Delta^{13}C_{c\text{-}DIC}$ (Fig. 5; Bolton and Stoll, 2013; McClelland et al., 2017). While vital effects are present with clear differences between *Gephyrocapsa* and *Calcidiscus*, further physiological explanations are outside the scope of this study.

4.2 Oxygen isotope vital effects in coccolith calcite

At a given temperature, equilibrium oxygen isotope fractionation between calcite and water is inferred to be represented by natural precipitation featuring very slow growth rates (Coplen, 2007; Daëron et al., 2019) or laboratory experiments using carbonic anhydrase (CA) to maintain oxygen isotopic exchange between DIC and H_2O (Watkins et al., 2013; 2014). This fractionation is illustrated as the 'equilibrium limit' in Fig. 3. Non-equilibrium fractionation effects that manifest at faster growth rates in experiments both with and without CA include lower $\Delta^{18}O_{c\text{-}w}$, and a pH-dependence. This effect presumably occurs because calcite forms from both bicarbonate and carbonate ions in proportion to their abundance in solution. At a higher pH the proportion of calcite carbon derived from the carbonate ion increases (McConnaughey, 1989; Clark et al., 1992; Dietzel et al., 1992; Zeebe and Wolf-Gladrow, 2001; Watkins et al., 2014; Devriendt et al., 2017). This process is illustrated by the 'kinetic limit' in Fig. 3. Additionally, numerous experiments and potentially many natural biogenic and abiogenic systems may precipitate calcite from a solution in which equilibrium between DIC and H_2O is not maintained due to a lack of CA or fast calcification rates (Devriendt et al., 2017; Daëron et al. 2019). Rayleigh fractionation of oxygen isotopes in the internal DIC pool occurs as a result, which is transferred to the isotopic composition of the calcite and leads to lower $\Delta^{18}O_{c\text{-}w}$ values. Recent studies suggest that in certain systems such as synthetically precipitated calcite, oxygen isotope disequilibrium does not affect Δ_{47}, even for systems with intermediate oxygen isotope fractionations that fall between the kinetic and equilibrium limits, as seen in Fig. 3 (Kelson et al., 2017; Levitt et al., 2018; Jautzy et al., 2020; Fiebig et al., 2021). Models also suggest this for biogenic carbonates such as foraminifera and bivalves, as the magnitude of potential Δ_{47} disequilibrium is below the current analytical resolution for Δ_{47} measurements (Defliese and Lohmann, 2015; Watkins and Hunt, 2015; Devriendt et al.,

https://doi.org/10.5194/egusphere-2023-2581
Preprint. Discussion started: 9 November 2023

2017). However, this does not hold for corals, brachiopods, and speleothems, where systematic $\delta^{18}O$ and Δ_{47} disequilibria are present (Watkins and Hunt, 2015; Guo and Zhou, 2019, Guo, 2020).

Offsets from the equilibrium limit ($\Delta\Delta^{18}O_{off}$) were calculated to quantify the vital effect in oxygen isotopes. Offsets may potentially arise from pH variability, growth rate, calcification rate, or disequilibrium within the DIC-H_2O system. *Calcidiscus* is significantly different from equilibrium (t-test; t(4) = -58.68, p-value <0.05) and falls outside the equilibrium and kinetic limits as seen in Fig. 3. Although for *Gephyrocapsa* the mean $\Delta\Delta^{18}O_{off}$ value is around zero and there is no significant difference from the abiogenically defined equilibrium (t-test; t(72) = -0.47, p-value = 0.64), there is a range of ~1.5‰ in $\Delta\Delta^{18}O_{off}$ among different experiments. Previously published *Gephyrocapsa* data has a positive $\Delta\Delta^{18}O_{off}$ of 0-1‰ (Fig. 5; Ziveri et al., 2003; Hermoso et al., 2016).

CA has been suggested as a potential equilibration mechanism for both oxygen isotopes and Δ_{47} within the DIC-H_2O system. Even at an elevated pH, the equilibration time is shortened considerably for abiogenic carbonates precipitated in the presence of CA (Uchikawa and Zeebe, 2012; Kelson et al., 2017). A lack or low activity of CA can potentially cause the variable $\Delta\Delta^{18}O_{off}$ seen in our data. While the pH of the intracellular calcification site for coccoliths is not well constrained, there is experimental evidence for CA in the biomineralization pathway of *Emiliania huxleyi* (Zhang et al., 2021). Although CA has not been explicitly found in *Gephyrocapsa*, it is associated with the cytosol, chloroplast, or extracellularly in other coccolithophores (Nimer et al., 1994; Elzenga et al., 2000; Herfort et al., 2002; Rost et al., 2003). Furthermore, genes have been found associated with biomineralization and CA expression in *E. huxleyi* (Quinn et al., 2006; Soto et al., 2006; Richier et al., 2011). Models show a requirement of CA activity in the calcification pathway of coccolithophores, either in the cytosol or coccolith vesicle itself, as a purely uncatalyzed exchange would have too enriched carbon isotope values in the coccolith calcite (Holtz et al., 2015; McClelland et al., 2017). Thus, it is probable that CA is present in coccolithophores. However, the activity of CA is not well constrained so it remains uncertain whether it is sufficient to ensure full equilibration of the DIC-H_2O system for both oxygen isotopes and Δ_{47}.

For *Gephyrocapsa*, the 1.5‰ range in $\Delta\Delta^{18}O_{off}$ also did not correlate with pH, growth rate, DIC, $CO_{2(aq)}$, or τ (Figs. S4, S5; Table S2). The 1.5‰ range in $\Delta\Delta^{18}O_{off}$ may be explained by varying degrees of isotopic equilibration between the DIC pool and intracellular water in different experiments. Non-systematic disequilibria effects could be present for our continuous culture setup as the equilibration time for oxygen isotopic exchange between our bubbled CO_2 gas and the seawater media is in the order of hours (Zeebe and Wolf-Gladrow, 2001; Uchikawa and Zeebe, 2012). In support of this interpretation, there is a difference of ~0.5‰ between all continuous and batch culture $\Delta\Delta^{18}O_{off}$ (t-test; t(38) = 1.76, p-value = 0.09, Fig. 5, Table S1). Further variability in $\Delta\Delta^{18}O_{off}$ could be a result of variable intracellular pH and/or varying calcification rates as well as the presence and activity of CA. However, these physiological variations do not exhibit systematic relationships with the individual environmental parameters such as growth rate, external pH, or carbonate system. This suggests a potential for complex co-regulation of the physiological factors and/or multiple environmental controls, which are best evaluated by cellular models.

https://doi.org/10.5194/egusphere-2023-2581
Preprint. Discussion started: 9 November 2023

4.3 Calibration of coccolith clumped isotopes and temperature

Despite the significant vital effects in carbon and oxygen isotopes, our coccolith Δ_{47} values show a consistent relationship with temperature (Fig. 6), and is similar to previous calibration studies (see Sect. 4.4). In order to calculate a reliable coccolith Δ_{47}-temperature regression, we used a bivariate least-squares fitting following Williamson (1968) and York et al. (2004), using the Excel spreadsheet by Cantrell (2008). This methodology considers the uncertainties from both the Δ_{47} and temperature measurements. However, as pointed out in a number of studies (Bonifacie et al., 2017; Fernandez et al., 2017; Katz et al., 2017; Kelson et al., 2017), the bias from a low number of analytical replicates and the small temperature range can lead to significant differences in calibration slope and intercepts. Thus, as *G. oceanica* contains the most diverse and largest range of datapoints, the other two species' datasets will be successively included and evaluated for significance. Further, each Δ_{47} measurement and uncertainty is taken individually as to have an equal contribution of each datapoint to the final calibration. The initial uncertainty of 0.1°C for temperature is 0.018 K^{-2} after conversion to $1/T^2$. The resulting slopes and intercepts of the Δ_{47}-temperature regressions are seen in Table 2. With the successive inclusion of the two other species, there is no significant change or offset in slope or intercept. All regression lines fall within error of each other, which shows there is no species- or genus-specific vital effect on the Δ_{47}-temperature relationship.

Secondly, we tested the potential influence of variable carbonate chemistry on the Δ_{47}-temperature relationship. To this end, we normalized our Δ_{47} data against the Meinicke et al. (2020) Δ_{47}-temperature calibration at each temperature to generate residual values ($\Delta\Delta_{47,off}$). Pearson correlation tests were then performed for the normalized $\Delta\Delta_{47,off}$ residual values against the different carbonate chemistry parameters. The resulting Pearson correlation coefficients are shown in Table 3. Apart from a weak positive and negative correlation for the batch and continuous culture setup and pH respectively, there are no conclusive or significant correlations for all measurements and experimental setups. Any difference in Δ_{47} as a result of the two culture setups; continuous and batch, must also be established. There is no significant difference in the normalized $\Delta\Delta_{47,off}$ values between batch and continuous culture setups (t-test; $t(38) = 0.35$, p-value = 0.73), further indicating that carbonate chemistry does not have an effect on the measured Δ_{47} value.

Thirdly, average Δ_{47} values were calculated for each species at every growth temperature. These temperature-weighted averages can highlight bias from a low number of measurement replicates at certain growth temperatures, such as at 6°C and 27°C. The resulting Δ_{47}-temperature regression is indistinguishable from regressions using individual datapoints (Table 2).

Lastly, if there are no species-specific nor carbonate chemistry related vital effects in the Δ_{47}-temperature relationship, the data that were initially excluded due to the poorly characterized carbonate system (see Sect. 3.1.1) and poor constraining of the stable carbon and oxygen isotope fractionations (i.e. datapoints with $\Delta_{DIC} \geq 20\%$ or $\Delta_{pH} \geq 0.20$) can also be included. If the Δ_{47}-temperature relationship in coccoliths is purely related to temperature, this will not interfere with the resulting calibration. Indeed, the slope and intercept fall within error of the other regressions, albeit with a slightly higher slope and lower intercept, seen in Table 2 and Fig. 6.

https://doi.org/10.5194/egusphere-2023-2581
Preprint. Discussion started: 9 November 2023

Based on the above analysis we conclude that all 55 datapoints can be considered for a coccolith Δ_{47}-temperature calibration (T in K, ±1σ):

$$\Delta_{47}(\mathrm{I-CDES}) = 0.0375 \pm 0.004 * \frac{10^6}{T^2} + 0.181 \pm 0.048 \quad (4)$$

4.4 A unified coccolith Δ_{47}-temperature calibration?

The similar culturing study of three coccolithophore species by Katz et al. (2017) also found no species-specific vital effects affecting the Δ_{47} values and a consistent Δ_{47}-temperature correlation. Furthermore, two common coccolithophore species (*E. huxleyi* and *C. braarudii*) were cultured that were not included in our study. Comparable and overlapping Δ_{47} values were obtained for all temperatures. If we combine the clumped isotope data from this study and Katz et al. (2017) (Fig. 7) we obtain a coccolith Δ_{47}-temperature calibration that falls within the 95% confidence interval of Eq. 4:

$$\Delta_{47}(\mathrm{I-CDES}) = 0.0381 \pm 0.003 * \frac{10^6}{T^2} + 0.176 \pm 0.037 \quad (5)$$

However, the study was conducted before the introduction of the I-CDES standardisation methodology using carbonates and used gas-based standardization, consequently the data could have a systematic difference that cannot be resolved with certainty. Thus, when comparing to other calibration studies we will not include Katz et al. (2017) in the dataset and use Eq. 4 as a coccolith Δ_{47}-temperature calibration, which is only based on our culture data in the I-CDES frame.

4.5 Comparison with other calibrations

In Fig. 8 we compare our data with the individual data of previous Δ_{47}-temperature calibration studies. The slopes and the intercepts of the equations with a limited number of replicates and a limited range of temperatures have larger uncertainties (Bonifacie et al., 2017; Fernandez et al., 2017; Kelson et al., 2017) and all datasets have a significant scatter due to their small variability. We focus on three biogenic and one inorganic carbonate calibration studies (Peral et al., 2018; Meinicke et al., 2020; Anderson et al., 2021; de Winter et al., 2022). We also include the 'MIT calibration' equation of Daëron and Gray (2023), however as no new data was generated in that study only the recalculated calibration curve is shown. All datasets are converted to I-CDES using the methodology described in Bernasconi et al. (2021) and seen in Fig. 8.

While overall the Δ_{47} values for coccolith calcite fall within the scatter of the Peral et al. (2018) and Meinicke et al. (2020) calibrations, our coccolith Δ_{47}-temperature calibration plots slightly above previous calibrations, but generally below Katz et al. (2017). To identify and evaluate how this would impact temperature reconstructions, a similar exercise to Sect. 4.3 was performed. At all growth temperatures, a Δ_{47} value was calculated from each calibration. $\Delta\Delta_{47,\mathrm{off}}$ residuals were then generated through comparison with our study's calibration at each temperature.

Katz et al. (2017) yield positive residuals whereas the non-coccolith calibrations yield negative residuals ($\Delta\Delta_{47,\mathrm{off}}$) relative to our coccolith Δ_{47}-temperature calibration (Fig. 9). This results in lower calculated Δ_{47} temperatures compared to our calibration. Similar results were found for aragonite and brachiopods by de Winter et al. (2022) and Letulle et al. (2023) respectively, when compared to the Anderson et al. (2021) calibration. de Winter et al. (2022) argued that the Δ_{47}-temperature

https://doi.org/10.5194/egusphere-2023-2581
Preprint. Discussion started: 9 November 2023

relationship is non-linear and calibrations are substantially biased by data with a large temperature range such as Anderson et al. (2021). Indeed, applying the Anderson et al. (2021) calibration yields lower and non-overlapping $\Delta\Delta_{47,off}$ residuals relative to our calibration, see Table 4 and Fig. 9. Using only the data <30°C from Anderson et al. (2021) to calculate a temperature regression does yield overlapping $\Delta\Delta_{47,off}$ residuals, however it is strongly temperature dependent (see Table S1). Yet, Letulle et al. (2023) argues against this bias from warmer temperatures and shows that their offsets are similar for calibrations derived from the marine temperature realm (<30°C). Offsets are instead most likely due to the uncertainty related to imprecise calcification temperatures in previous calibrations. Often indirectly inferred or estimated from other proxies, these uncertainties in the calcification temperatures can result in large variabilities, obscure potential effects related to temperature, and can result in small absolute differences between calibrations (see Daëron and Gray, 2023 for discussion). Both the variability and absolute $\Delta\Delta_{47,off}$ residuals differ for all compared calibrations. Katz et al. (2017), Anderson et al. (2021), and Daëron and Gray (2023) yield $\Delta\Delta_{47,off}$ residuals that do not overlap with our dataset. Peral et al. (2018), Meinicke et al. (2020), and de Winter et al. (2022) yield $\Delta\Delta_{47,off}$ residuals within the uncertainty of our dataset, see Table 4 and Fig. 9. Temperature offsets at the average growth temperature of our dataset, 18.7°C, are between -3°C and 3°C for the different calibrations, although vary in magnitude at different temperatures, see Table 4 and Fig. 9.

Our tightly-controlled growth temperatures of the culture data eliminate the problem of uncertain calcification temperatures as in the case of foraminifera calibrations (Meinicke et al., 2020; Daëron and Gray, 2023). It also allows the exclusion of effects from environmental variabilities, such as pCO_2, pH, growth rate, and vital effects on measured Δ_{47} values as discussed in Sect. 4.3. It is important to note that the vital effects in the coccolith carbon and oxygen isotopes have no impact on their Δ_{47}. Furthermore, modelling studies for inorganic calcite, grown in the presence of CA and at growth rates and pH ranges relevant for coccolithophores, also show clear vital effects for carbon and oxygen but find no distinction between equilibrium and modelled Δ_{47} (Watkins and Hunt, 2015; Hill et al., 2020; Uchikawa et al., 2021; Watkins and Devriendt, 2022). While all compared biogenic calibrations fall within ±1°C of this studies' calibration, the inorganic carbonate calibrations yield systematically colder temperatures by at least 2°C (Fig. 9a, c). As our study was performed with strict temperature regulation, any related uncertainty can be eliminated as a source of inter-calibration variability. As all compared biogenic carbonates are within uncertainty of our study, we suggest that a constant biological mechanism is causing the offset of biogenic relative to inorganic carbonates. A combination of all data from Peral et al. (2018), Meinicke et al. (2020), de Winter et al. (2022), and this study yields a general biogenic Δ_{47}-temperature calibration (Eq. 6; Fig. 9b).

$$\Delta_{47}(\mathrm{I-CDES}) = 0.0371 \pm 0.001 * \frac{10^6}{T^2} + 0.184 \pm 0.016 \quad (6)$$

All previous biogenic calibrations fall within ±1°C and the 95% confidence interval of the general biogenic calibration (Fig. 9b). Thus, when reconstructing calcification temperatures from biogenic carbonates, we suggest the use of a well-constrained and biogenic specific calibration such as Eq. 4.

https://doi.org/10.5194/egusphere-2023-2581
Preprint. Discussion started: 9 November 2023

5 Conclusions

In this study we cultured three species of coccolithophores (*Gephyrocapsa oceanica*, *G. muellerae*, and *Calcidiscus leptoporus*) in continuous and batch culture setups for temperatures between 6 and 27°C and $CO_{2(aq)}$ between 5 and 45 µM. Vital effects in carbon and oxygen isotopes in coccoliths were observed and their magnitude is consistent with previous culturing studies. We show that for our well-constrained continuous culture setup there are no systematic external environmental influences from pH, DIC, or $CO_{2(aq)}$ on the carbon and oxygen isotopic values for both *G. oceanica* and *G. muellerae*. Both species precipitate coccolith calcite close to isotopic equilibrium with the water. *C. leptoporus* shows pronounced vital effects in both carbon and oxygen isotopes, although no clear physiological conclusions can be drawn on the source of these vital effects.

We establish a coccolith-specific Δ_{47}-temperature calibration and find no distinguishable vital effects in coccolith Δ_{47} for all three coccolithophore species. There are also no effects due to differences in environmental parameters. Our coccolith Δ_{47} data is largely consistent with a previous coccolith culture study (Katz et al., 2017), and indicates that coccolithophores precipitate coccolith calcite in clumped isotope equilibrium with their environment. Our well-constrained coccolith Δ_{47}-temperature calibration (Eq. 4) shows no consistent offset from previous biogenic calibration studies (≤2°C). Combining the previous biogenic calibrations into a general Δ_{47}-temperature calibration (Eq. 6) yields better constraints and no consistent offsets between calibrations (±2°C). However, there is a systematic offset of ≥2°C from previous inorganic calibrations. Thus, while all previous biogenic calibrations can be used interchangeably, we suggest the use of our well-constrained Δ_{47}-temperature calibration to reconstruct temperatures from well screened/preserved coccolith calcite.

Author contributions.

AJC: cell culture, analyses, and writing, ITR: cell culture and analyses, MJ: analyses, SMB: supervision, analyses, funding acquisition, and writing, HMS: supervision, funding acquisition, and writing.

Competing interests

The authors declare that they have no conflict of interest.

Acknowledgements

The authors thank Anne-Greet Bittermann of ScopeM for their support and assistance in this work. This work was supported by ETH core funding.

https://doi.org/10.5194/egusphere-2023-2581
Preprint. Discussion started: 9 November 2023

References

Anderson, N., Kelson, J., Kele, S., Daëron, M., Bonifacie, M., Horita, J., Mackey, T., John, C., Kluge, T., Petschnig, P., Jost, A., Huntington, K., Bernasconi, S., Bergmann, K.: A Unified Clumped Isotope Thermometer Calibration (0.5–1,100°C) Using Carbonate-Based Standardization, Geophys Res Lett, 48(7), 10.1029/2020GL092069, 2021.

Bach, L., MacKinder, L., Schulz, K., Wheeler, G., Schroeder, D., Brownlee, C., and Riebesell, U.: Dissecting the impact of CO2 and pH on the mechanisms of photosynthesis and calcification in the coccolithophore Emiliania huxleyi, New Phytol, 199(1), 121-134, 10.1111/nph.12225, 2013.

Barry, J., Hall-Spencer, J., and Tyrrell, T.: In situ perturbation experiments: natural venting sites, spatial/temporal gradients in ocean pH, manipulative in situ pCO2 perturbations, in: Guide to best practices for ocean acidification research and data reporting, edited by: U. Riebesell, V. Fabry, L. Hansson, and Gattuso J.-P., Office for Official Publications of the European Communities, Luxembourg, 123-136, 10.2777/66906, 2012.

Berger, W.: Deep-sea carbonates: evidence for a coccolith lysocline, Deep-Sea Res, 20, 917-921, 1973.

Berman, A., Hanson, J., Leiserowitz, L., Koetzle, T., Weiner, S., and Addadi, B.: Biological Control of Crystal Texture: A Widespread Strategy for Adapting Crysta Properties to Function, Science, 259, 776-779, 10.1126/science.259.5096.776, 1993.

Bernasconi, S., Hu, B., Wacker, U., Fiebig, J., Breitenbach, S., and Rutz, T.: Background effects on Faraday collectors in gas-source mass spectrometry and implications for clumped isotope measurements. Rapid Commun Mass Sp, 27(5), 603-612, 10.1002/rcm.6490, 2013.

Bernasconi, S., Müller, I., Bergmann, K., Breitenbach, S., Fernandez, A., Hodell, D., Jaggi, M., Meckler, A., Millan, I., and Ziegler, M.: Reducing Uncertainties in Carbonate Clumped Isotope Analysis Through Consistent Carbonate-Based Standardization, Geochem Geophy Geosy, 19(9), 2895-2914, 10.1029/2017GC007385, 2018.

Bernasconi, S., Daëron, M., Bergmann, K., Bonifacie, M., Meckler, A., Affek, H., Anderson, N, Bajnai, D., Barkan, E., Beverly, E., Blamart, D., Burgener, L., Calmels, D., Chaduteau, C., Clog, M., Davidheiser-Kroll, B., Davies, A., Dux, F., Eiler, J., Elliott, B., Fetrow, A.C., Fiebig, J., Goldberg, S., Hermoso, M., Huntington, K.W., Hyland, E., Ingalls, M., Jaggi, M., John, C.M., Jost, A.B., Katz, S., Kelson, J., Kluge, T., Kocken, I.J., Laskar, A., Leutert, T.J., Liang, D., Lucarelli, J., Mackey, T.J., Mangenot, X., Meinicke, N., Modestou, S.E., Muller, I.A., Murray, S., Neary, A., Packard, N., Passey, B.H., Pelletier, E., Petersen, S., Piasecki, A., Schauer, A., Snell, K.E., Swart, P.K., Tripati, A., Upadhyay, D., Vennemann, T., Winkelstern, I., Yarian, D., Yoshida, N., Zhang, N., and Ziegler, M.: InterCarb: A Community Effort to Improve Interlaboratory Standardization of the Carbonate Clumped Isotope Thermometer Using Carbonate Standards, Geochem, Geophy, Geosy, 22(5), 10.1029/2020GC009588, 2021.

Blanco-Ameijeiras, S., Stoll, H., Zhang, H., and Hopkinson, B.: Influence of temperature and CO2 on plasma-membrane permeability to CO2 and HCO3- in the marine haptophytes Emiliania huxleyi and Calcidiscus leptoporus (Prymnesiophyceaea), J Phycol, 56, 1283-1294, doi/10.1111/jpy.13017, 2020.

https://doi.org/10.5194/egusphere-2023-2581
Preprint. Discussion started: 9 November 2023

Bolton, C., and Stoll, H.: Late Miocene threshold response of marine algae to carbon dioxide limitation, Nature, 500(7464), 558-562, 10.1038/nature12448, 2013.

Bonifacie, M., Calmels, D., Eiler, J., Horita, J., Chaduteau, C., Vasconcelos, C., Agrinier, P., Katz, A., Passey, B., Ferry, J., and Bourrand, J.: Calibration of the dolomite clumped isotope thermometer from 25 to 350 °C, and implications for a universal calibration for all (Ca, Mg, Fe)CO3 carbonates, Geochim Cosmochim Ac, 200, 255-279, 10.1016/j.gca.2016.11.028, 2017.

Candelier, Y., Minoletti, F., Probert, I., and Hermoso, M.: Temperature dependence of oxygen isotope fractionation in coccolith calcite: A culture and core top calibration of the genus Calcidiscus, Geochim Cosmochim Ac, 100, 264-281, 2013.

Cantrell, C.: Technical Note: Review of methods for linear least-squares fitting of data and application to atmospheric chemistry problems, Atmos Chem Phys, 8(17), 5477-5487, 10.5194/acp-8-5477-2008, 2008.

Clark, I., Fontes, J.-C., and Fritz, P.: Stable isotope disequilibria in travertine from high pH waters: Laboratory investigations and field observations from Oman, Geochim Cosmochim Ac, 56, 2041-2050, https://doi.org/10.1016/0016-7037(92)90328-G, 1992.

Coplen, T.: Calibration of the calcite-water oxygen-isotope geothermometer at Devils Hole, Nevada, a natural laboratory, Geochim Cosmochim Ac, 71(16), 3948-3957, 10.1016/j.gca.2007.05.028, 2007.

Daëron, M.: Full Propagation of Analytical Uncertainties in Δ47 Measurements, Geochem Geophy Geosy, 22(5), 10.1029/2020GC009592, 2021.

Daëron, M., and Gray, W.: Revisiting oxygen-18 and clumped isotopes in planktic and benthic foraminifera, Paleoceanography and Paleoclimatology, 38(10), 2023-2032, 10.1029/2023PA004660, 2023.

Daëron, M., Blamart, D., Peral, M., and Affek, H.: Absolute isotopic abundance ratios and the accuracy of Δ47 measurements, Chem Geol, 442, 83-96, 10.1016/j.chemgeo.2016.08.014, 2016.

Daëron, M., Drysdale, R., Peral, M., Huyghe, D., Blamart, D., Coplen, T., Lartaud, F., and Zanchetta, G.: Most Earth-surface calcites precipitate out of isotopic equilibrium, Nature Commun, 10(1), 10.1038/s41467-019-08336-5, 2019.

de Winter, N., Witbaard, R., Kocken, I., Müller, I., Guo, J., Goudsmit, B., and Ziegler, M.: Temperature Dependence of Clumped Isotopes (Δ47) in Aragonite, Geophys Res Lett, 49(20), 10.1029/2022GL099479, 2022.

Defliese, W., and Lohmann, K.: Non-linear mixing effects on mass-47 CO2 clumped isotope thermometry: Patterns and implications, Rapid Commun Mass Sp, 29(9), 901-909, 10.1002/rcm.7175, 2015.

Deng, X., Li, Q., Su, J., Liu, C., Atekwana, E., and Cai, W.: Performance evaluations and applications of a δ13C-DIC analyzer in seawater and estuarine waters, Sci Total Environ, 833, 10.1016/j.scitotenv.2022.155013, 2022.

Dennis, K., and Schrag, D.: Clumped isotope thermometry of carbonatites as an indicator of diagenetic alteration, Geochim Cosmochim Ac, 74(14), 4110-4122, 10.1016/j.gca.2010.04.005, 2010.

Devriendt, L., Watkins, J., and McGregor, H.: Oxygen isotope fractionation in the CaCO3-DIC-H2O system, Geochim Cosmochim Ac, 214, 115-142, 10.1016/j.gca.2017.06.022, 2017.

https://doi.org/10.5194/egusphere-2023-2581
Preprint. Discussion started: 9 November 2023

Dickson, A.: Standard potential of the reaction: AgCl(s) + 1/2H2(g) = Ag(s) + HCl(aq), and the standard acidity constant of the ion HSO4- in synthetic sea water from 273.15 to 318.15 K. J Chem Thermodyn, 22, 113-127, 10.1016/0021-9614(90)90074-Z, 1990.

Dietzel, M., Usdowski, E., and Hoefst, J.: Chemical and 13C/12C- and 18O/16O-isotope evolution of alkaline drainage waters and the precipitation of calcite, Appl Geochem, 7, 177-184, 10.1016/0883-2927(92)90035-2, 1992.

Drury, A., and John, C.: Exploring the potential of clumped isotope thermometry on coccolith-rich sediments as a sea surface temperature proxy, Geochem Geophy Geosy, 17(10), 4092-4104, 10.1002/2016GC006459, 2016.

Eiler, J.: "Clumped-isotope" geochemistry-The study of naturally-occurring, multiply-substituted isotopologues, Earth Planet Sc Lett, 262(3-4), 309-327, 10.1016/j.epsl.2007.08.020, 2007.

Eiler, J., and Schauble, E.: 18O13C16O in Earth's atmosphere, Geochim Cosmochim Ac, 68(23), 4767-4777, 10.1016/j.gca.2004.05.035, 2004.

Elzenga, J., Prins, H., and Stefels, J.: The role of extracellular carbonic anhydrase activity in inorganic carbon utilization of Phaeocystis globosa (Prymnesiophyceae): A comparison with other marine algae using the isotopic disequilibrium technique, Limnol Oceanogr, 45(2), 372-380, 10.4319/lo.2000.45.2.0372, 2000.

Falster, G., Delean, S., and Tyler, J.: Hydrogen Peroxide Treatment of Natural Lake Sediment Prior to Carbon and Oxygen Stable Isotope Analysis of Calcium Carbonate, Geochem Geophy Geosy, 19(9), 3583-3595, 10.1029/2018GC007575, 2018.

Fernandez, A., Müller, I., Rodríguez-Sanz, L., van Dijk, J., Looser, N., and Bernasconi, S.: A Reassessment of the Precision of Carbonate Clumped Isotope Measurements: Implications for Calibrations and Paleoclimate Reconstructions, Geochem Geophy Geosy, 18(12), 4375-4386, 10.1002/2017GC007106, 2017.

Fiebig, J., Daëron, M., Bernecker, M., Guo, W., Schneider, G., Boch, R., Bernasconi, S., Jautzy. J., Dietzel, M.: Calibration of the dual clumped isotope thermometer for carbonates, Geochim Cosmochim Ac, 312, 235-256, 10.1016/j.gca.2021.07.012, 2021.

Frølich, S., Sørensen, H., Hakim, S., Marin, F., Stipp, S., and Birkedal, H.: Smaller calcite lattice deformation caused by occluded organic material in coccoliths than in mollusk shell, Cryst Growth Des, 15(6), 2761-2767, 10.1021/acs.cgd.5b00118, 2015.

Ghosh, P., Adkins, J., Affek, H., Balta, B., Guo, W., Schauble, E., Schrag, D., Eiler, J.: 13C-18O bonds in carbonate minerals: A new kind of paleothermometer, Geochim Cosmochim Ac, 70(6), 1439-1456, 10.1016/j.gca.2005.11.014, 2006.

Guo, W.: Kinetic clumped isotope fractionation in the DIC-H2O-CO2 system: Patterns, controls, and implications, Geochim Cosmochim Ac, 268, 230-257, 10.1016/j.gca.2019.07.055, 2020.

Guo, W., and Zhou, C.: Patterns and controls of disequilibrium isotope effects in speleothems: Insights from an isotope-enabled diffusion-reaction model and implications for quantitative thermometry, Geochim Cosmochim Ac, 267, 196-226, 10.1016/j.gca.2019.07.028, 2019.

https://doi.org/10.5194/egusphere-2023-2581
Preprint. Discussion started: 9 November 2023

Gupta, P., Noone, D., Galewsky, J., Sweeney, C., and Vaughn, B.: Demonstration of high-precision continuous measurements of water vapor isotopologues in laboratory and remote field deployments using wavelength-scanned cavity ring-down spectroscopy (WS-CRDS) technology, Rapid Commun Mass Sp, 23(16), 2534-2542, 10.1002/rcm.4100, 2009.

Henriksen, K., Young, J., Brown, P., & Stipp, S.: Coccolith biomineralisation studied with atomic force microscopy, Palaeontology, 47(3), 725-743, 10.1111/j.0031-0239.2004.00385.x, 2004.

Herfort, L., Thake, B., and Roberts, J.: Acquisition and use of bicarbonate by Emiliania huxleyi, New Phytol, 156(3), 427-436, 10.1046/j.1469-8137.2002.00523.x, 2002.

Hermoso, M.: Coccolith-derived isotopic proxies in palaeoceanography: Where geologists need biologists, Cryptogamie, Algol, 35(4), 323-351, 10.7872/crya.v35.iss4.2014.323, 2014.

Hermoso, M., Horner, T., Minoletti, F., and Rickaby, R.: Constraints on the vital effect in coccolithophore and dinoflagellate calcite by oxygen isotopic modification of seawater, Geochim Cosmochim Ac, 141, 612-627, 10.1016/j.gca.2014.05.002, 2014.

Hermoso, M., Minoletti, F., Aloisi, G., Bonifacie, M., McClelland, H., Labourdette, N., Renforth, P., Chaduteau, C., and Rickaby, R.: An explanation for the 18O excess in Noelaerhabdaceae coccolith calcite, Geochim Cosmochim Ac, 189, 132-142, 10.1016/j.gca.2016.06.016, 2016.

Hill, P., Schauble, E., and Tripati, A.: Theoretical constraints on the effects of added cations on clumped, oxygen, and carbon isotope signatures of dissolved inorganic carbon species and minerals, Geochim Cosmochim Ac, 269, 496-539, 10.1016/j.gca.2019.10.016, 2020.

Holtz, L., Wolf-Gladrow, D., and Thoms, S.: Simulating the effects of light intensity and carbonate system composition on particulate organic and inorganic carbon production in Emiliania huxleyi, J Theor Biol, 372, 192-204, 10.1016/j.jtbi.2017.01.030, 2015.

Holtz, L., Wolf-Gladrow, D., and Thoms, S.: Stable carbon isotope signals in particulate organic and inorganic carbon of coccolithophores – A numerical model study for Emiliania huxleyi, J Theor Biol, 420, 117-127, 10.1016/j.jtbi.2015.02.024, 2017.

Houdan, A., Probert, I., Zatylny, C., Véron, B., and Billard, C.: Ecology of oceanic coccolithophores. I. Nutritional preferences of the two stages in the life cycle of Coccolithus braarudii and Calcidiscus leptoporus, Aquat Microb Ecol, 44, 291-301, 10.3354/ame044291, 2006.

Hu, B., Radke, J., Schlüter, H., Heine, F., Zhou, L., and Bernasconi, S.: A modified procedure for gas-source isotope ratio mass spectrometry: The long-integration dual-inlet (LIDI) methodology and implications for clumped isotope measurements, Rapid Commun Mass Sp, 28(13), 1413-1425, 10.1002/rcm.6909, 2014.

Huntington, K., and Petersen, S.: Frontiers of Carbonate Clumped Isotope Thermometry, Annu Rev Earth Pl Sc, 51, 611-41, 10.1146/annurev-earth-031621, 2023.

Huyghe, D., Daëron, M., de Rafelis, M., Blamart, D., Sébilo, M., Paulet, Y., and Lartaud, F.: Clumped isotopes in modern marine bivalves, Geochim Cosmochim Ac, 316, 41-58, 10.1016/j.gca.2021.09.019, 2022.

https://doi.org/10.5194/egusphere-2023-2581
Preprint. Discussion started: 9 November 2023

Jautzy, J., Savard, M., Dhillon, R., Bernasconi, S., & Smirnoff, A. (2020). Clumped isotope temperature calibration for calcite: Bridging theory and experimentation, Geochem Perspect Lett, 10.7185/geochemlet.2021, 2020.

John, C., and Bowen, D.: Community software for challenging isotope analysis: First applications of 'Easotope' to clumped isotopes, Rapid Commun Mass Sp, 30(21), 2285-2300, 10.1002/rcm.7720, 2016.

Katz, A., Bonifacie, M., Hermoso, M., Cartigny, P., and Calmels, D.: Laboratory-grown coccoliths exhibit no vital effect in clumped isotope (Δ47) composition on a range of geologically relevant temperatures, Geochim Cosmochim Ac, 208, 335-353, 10.1016/j.gca.2017.02.025ï, 2017.

Kele, S., Breitenbach, S., Capezzuoli, E., Meckler, A., Ziegler, M., Millan, I., Kluge, T., Deak, J., Hanselmann, K., John, C., Yan, H., Liu, Z., Bernasconi, S.: Temperature dependence of oxygen- and clumped isotope fractionation in carbonates: A study of travertines and tufas in the 6-95°C temperature range, Geochim Cosmochim Ac, 168, 172-192, 10.1016/j.gca.2015.06.032, 2015.

Keller, M., Seluin, R., Claus, W., and Guillard, R.: Media for the culture of oceanic ultraphytoplankton, J Phycol, 23, 633-638, https://doi.org/10.1111/j.1529-8817.1987.tb04217.x, 1987.

Kelson, J., Huntington, K., Schauer, A., Saenger, C., and Lechler, A.: Toward a universal carbonate clumped isotope calibration: Diverse synthesis and preparatory methods suggest a single temperature relationship, Geochim Cosmochim Ac, 197, 104-131, 10.1016/j.gca.2016.10.010, 2017.

Kester, D., Duedall, I., Connors, D., and Pytkowicz, R.: Preparation of Artificial Seawater, Limnol Oceanogr, 12(1), 176-179, 10.4319/lo.1967.12.1.0176, 1967.

Langer, G., Oetjen, K., and Brenneis, T.: Calcification of Calcidiscus leptoporus under nitrogen and phosphorus limitation, J Exp Mar Biol Ecol, 413, 131-137, 10.1016/j.jembe.2011.11.028, 2012.

Lee, K., Kim, T., Byrne, R., Millero, F., Feely, R., and Liu, Y.: The universal ratio of boron to chlorinity for the North Pacific and North Atlantic oceans, Geochim Cosmochim Ac, 74(6), 1801-1811, 10.1038/ncomms13144, 2010.

Lee, R., Mavridou, D., Papadakos, G., McClelland, H., and Rickaby, R.: The uronic acid content of coccolith-associated polysaccharides provides insight into coccolithogenesis and past climate, Nature Commun, 7, 10.1016/j.gca.2009.12.027, 2016.

Letulle, T., Gaspard, D., Daëron, M., Arnaud-Godet, F., Vinçon-Laugier, A., Suan, G., and Lécuyer, C.: Multi-proxy assessment of brachiopod shell calcite as a potential archive of seawater temperature and oxygen isotope composition, Biogeosciences, 20(7), 1381-1403, 10.5194/bg-20-1381-2023, 2023.

Leuker, T., Dickson, A., and Keeling, C.: Ocean pCO2 calculated from dissolved inorganic carbon, alkalinity, and equations for K1 and K2: validation based on laboratory measurements of CO2 in gas and seawater at equilibrium, Mar Chem, 70, 105-119, 10.1016/S0304-4203(00)00022-0, 2000.

Leutert, T., Sexton, P., Tripati, A., Piasecki, A., Ho, S., and Meckler, A.: Sensitivity of clumped isotope temperatures in fossil benthic and planktic foraminifera to diagenetic alteration, Geochim Cosmochim Ac, 257, 354-372, 10.1016/j.gca.2019.05.005, 2019.

https://doi.org/10.5194/egusphere-2023-2581
Preprint. Discussion started: 9 November 2023

Levitt, N., Eiler, J., Romanek, C., Beard, B., Xu, H., and Johnson, C.: Near Equilibrium 13C-18O Bonding During Inorganic Calcite Precipitation Under Chemo-Stat Conditions, Geochem Geophy Geosy, 19(3), 901-920, 10.1002/2017GC007089, 2018.

Lewis, E., and Wallace, D.: Program Developed for CO2 System Calculations, 10.15485/1464255, 1998.

Matyash, V., Liebisch, G., Kurzchalia, T., Shevchenko, A., and Schwudke, D.: Lipid extraction by methyl-terf-butyl ether for high-throughput lipidomics, J Lipid Res, 49(5), 1137-1146, 10.1194/jlr.D700041-JLR200, 2008.

McClelland, H., Bruggeman, J., Hermoso, M., and Rickaby, R.: The origin of carbon isotope vital effects in coccolith calcite, Nature Commun, 8, 10.1038/ncomms14511, 2017.

McConnaughey, T.: 13C and 18O isotopic disequilibrium in biological carbonates: II. in vitro simulation of kinetic isotope effects, Geochim Cosmochim Ac, 53, 163-171, https://doi.org/10.1016/0016-7037(89)90283-4, 1989.

Meckler, A., Ziegler, M., Millán, M., Breitenbach, S., and Bernasconi, S.: Long-term performance of the Kiel carbonate device with a new correction scheme for clumped isotope measurements, Rapid Commun Mass Sp, 28(15), 1705-1715, 10.1002/rcm.6949, 2014.

Meinicke, N., Ho, S., Hannisdal, B., Nürnberg, D., Tripati, A., Schiebel, R., and Meckler, A.: A robust calibration of the clumped isotopes to temperature relationship for foraminifers, Geochim Cosmochim Ac, 270, 160-183, 10.1016/j.gca.2019.11.022, 2020.

Moolna, A., and Rickaby, R.: Interaction of the coccolithophore Gephyrocapsa oceanica with its carbon environment: Response to a recreated high-CO2 geological past, Geobiology, 10(1), 72-81, 10.1111/j.1472-4669.2011.00308.x, 2012.

Müller, I., Fernandez, A., Radke, J., van Dijk, J., Bowen, D., Schwieters, J., and Bernasconi, S.: Carbonate clumped isotope analyses with the long-integration dual-inlet (LIDI) workflow: scratching at the lower sample weight boundaries, Rapid Commun Mass Sp, 31(12), 1057-1066, 10.1002/rcm.7878, 2017.

Müller, I., Rodriguez-Blanco, J., Storck, J., do Nascimento, G., Bontognali, T., Vasconcelos, C., Benning, L., Bernasconi, S.: Calibration of the oxygen and clumped isotope thermometers for (proto-)dolomite based on synthetic and natural carbonates, Chem Geol, 525, 1-17, 10.1016/j.chemgeo.2019.07.014, 2019.

Nimer, N., Guan, Q., and Merrett, M.: Extra- and intra-cellular carbonic anhydrase in relation to culture age in a high-calcifying strain of Emiliania huxleyi Lohmann, New Phytol, 126(4), 601-607, 10.1111/j.1469-8137.1994.tb02954.x, 1994.

Peral, M., Daëron, M., Blamart, D., Bassinot, F., Dewilde, F., Smialkowski, N., Isguder, G., Bonnin, J., Jorissen, F., Kissel, C., Michel, E., Vazquez Riveiros, N., Waelbroeck, C.: Updated calibration of the clumped isotope thermometer in planktonic and benthic foraminifera, Geochim Cosmochim Ac, 239, 1-16, 10.1016/j.gca.2018.07.016, 2018.

Perez, F., and Fraga, F.: Association Constant of Fluoride and Hydrogen ions in seawater, Mar Chem, 21, 168, https://doi.org/10.1016/0304-4203(87)90036-3, 1987.

Phelps, S., Stoll, H., Bolton, C., Beaufort, L., and Polissar, P.: Controls on Alkenone Carbon Isotope Fractionation in the Modern Ocean, Geochem Geophy Geosy, 22(12), 10.1029/2021GC009658, 2021.

https://doi.org/10.5194/egusphere-2023-2581
Preprint. Discussion started: 9 November 2023

Piasecki, A., Bernasconi, S., Grauel, A., Hannisdal, B., Ho, S., Leutert, T., Marchitto, T., Meinicke, N., Tisserand, A., and Meckler, N.: Application of Clumped Isotope Thermometry to Benthic Foraminifera, Geochem Geophy Geosy, 20(4), 2082-2090, 10.1029/2018GC007961, 2019.

Quinn, P., Bowers, R., Zhang, X., Wahlund, T., Fanelli, M., Olszova, D., and Read, B.: cDNA microarrays as a tool for identification of biomineralization proteins in the coccolithophorid Emiliania huxleyi (Haptophyta), Appl Environ Microb, 72(8), 5512-5526, 10.1128/AEM.00343-06, 2006.

Richier, S., Fiorini, S., Kerros, M., von Dassow, P., and Gattuso, J.: Response of the calcifying coccolithophore Emiliania huxleyi to low pH/high pCO2: From physiology to molecular level, Mar Biol, 158(3), 551-560, 10.1007/s00227-010-1580-8, 2011.

Rickaby, R., Henderiks, J., and Young, J.: Perturbing phytoplankton: Response and isotopic fractionation with changing carbonate chemistry in two coccolithophore species, Clim Past, 6(6), 771-785, 10.5194/cp-6-771-2010, 2010.

Rost, B., Riebesell, U., Burkhardt, S., and Sültemeyer, D. (2003). Carbon acquisition of bloom-forming marine phytoplankton, Limnol Oceanogr, 48(1), 55-67, 10.4319/lo.2003.48.1.0055, 2003.

Sand, K., Pedersen, C., Sjöberg, S., Nielsen, J., Makovicky, E., and Stipp, S.: Biomineralization: Long-term effectiveness of polysaccharides on the growth and dissolution of calcite, Cryst Growth Des, 14(11), 5486-5494, 10.1021/cg5006743, 2014.

Schauble, E., Ghosh, P., and Eiler, J.: Preferential formation of 13C-18O bonds in carbonate minerals, estimated using first-principles lattice dynamics, Geochim Cosmochim Ac, 70(10), 2510-2529, 10.1016/j.gca.2006.02.011, 2006.

Sett, S., Bach, L., Schulz, K., Koch-Klavsen, S., Lebrato, M., and Riebesell, U.: Temperature modulates coccolithophorid sensitivity of growth, photosynthesis and calcification to increasing seawater pCO2, PLoS ONE, 9(2), 10.1371/journal.pone.0088308, 2014.

Soto, A., Zheng, H., Shoemaker, D., Rodriguez, J., Read, B., and Wahlund, T.: Identification and preliminary characterization of two cDNAs encoding unique carbonic anhydrases from the marine alga Emiliania huxleyi, Appl Environ Microb, 72(8), 5500-5511, 10.1128/AEM.00237-06, 2006.

Spooner, P., Guo, W., Robinson, L., Thiagarajan, N., Hendry, K., Rosenheim, B., and Leng, M.: Clumped isotope composition of cold-water corals: A role for vital effects?, Geochim Cosmochim Ac, 179, 123-141, 10.1016/j.gca.2016.01.023, 2016.

Stevenson, E., Hermoso, M., Rickaby, R., Tyler, J., Minoletti, F., Parkinson, I., Mokadem, F., and Burton, K.: Controls on stable strontium isotope fractionation in coccolithophores with implications for the marine Sr cycle, Geochim Cosmochim Ac, 128, 225-235, 10.1016/j.gca.2013.11.043, 2014.

Stoll, H., Ruiz Encinar, J., Ignacio Garcia Alonso, J., Rosenthal, Y., Probert, I., and Klaas, C.: A first look at paleotemperature prospects from Mg in coccolith carbonate: Cleaning techniques and culture measurements, Geochem Geophy Geosy, 2(5), 10.1029/2000GC000144, 2001.

Subhas, A., McCorkle, D., Quizon, A., McNichol, A., and Long, M.: Selective Preservation of Coccolith Calcite in Ontong-Java Plateau Sediments, Paleoceanography and Paleoclimatology, 34(12), 2141-2157, 10.1029/2019PA003731, 2019.

Thierstein, H., and Young, J. (Eds.): Coccolithophores, Springer Berlin Heidelberg, 10.1007/978-3-662-06278-4, 2004.

https://doi.org/10.5194/egusphere-2023-2581
Preprint. Discussion started: 9 November 2023

Uchikawa, J., and Zeebe, R.: The effect of carbonic anhydrase on the kinetics and equilibrium of the oxygen isotope exchange in the CO 2-H 2O system: Implications for δ 18O vital effects in biogenic carbonates, Geochim Cosmochim Ac, 95, 15-34, 10.1016/j.gca.2012.07.022, 2012.

Uchikawa, J., Chen, S., Eiler, J., Adkins, J., and Zeebe, R.: Trajectory and timescale of oxygen and clumped isotope equilibration in the dissolved carbonate system under normal and enzymatically-catalyzed conditions at 25 °C, Geochim Cosmochim Ac, 314, 313-333, 10.1016/j.gca.2021.08.014, 2021.

von Dassow, P., Muñoz Farías, P., Pinon, S., Velasco-Senovilla, E., and Anguita-Salinas, S.: Do Differences in Latitudinal Distributions of Species and Organelle Haplotypes Reflect Thermal Reaction Norms Within the Emiliania/Gephyrocapsa Complex?, Front Mar Sci, 8, 10.3389/fmars.2021.785763, 2021.

Walker, J., Marzec, B., Lee, R., Vodrazkova, K., Day, S., Tang, C., Rickaby, R., Nudelman, F.: Polymorph Selectivity of Coccolith-Associated Polysaccharides from Gephyrocapsa Oceanica on Calcium Carbonate Formation In Vitro, Adv Funct Mater, 29(1), 10.1002/adfm.201807168, 2019.

Watkins, J., and Devriendt, L.: A Combined Model for Kinetic Clumped Isotope Effects in the CaCO3-DIC-H2O System, Geochem Geophy Geosy, 23(8), 10.1029/2021GC010200, 2022.

Watkins, J., and Hunt, J.: A process-based model for non-equilibrium clumped isotope effects in carbonates, Earth Planet Sc Lett, 432, 152-165, 10.1016/j.epsl.2015.09.042, 2015.

Watkins, J., Nielsen, L., Ryerson, F., and DePaolo, D.: The influence of kinetics on the oxygen isotope composition of calcium carbonate, Earth Planet Sci Lett, 375, 349-360, 10.1016/j.epsl.2013.05.054, 2013.

Watkins, J., Hunt, J., Ryerson, F., and DePaolo, D.: The influence of temperature, pH, and growth rate on the δ18O composition of inorganically precipitated calcite, Earth Planet Sci Lett, 404, 332-343, 10.1016/j.epsl.2014.07.036, 2014.

Williamson, J.: Least-squares fitting of a straight line, Can J Phys, 18, 1845-1847, 10.1139/p68-523, 1968.

York, D., Evensen, N., Martínez, M., and De Basabe Delgado, J.: Unified equations for the slope, intercept, and standard errors of the best straight line, Am J Phys, 72(3), 367-375, 10.1119/1.1632486, 2004.

Zeebe, R., and Wolf-Gladrow, D.: CO2 in seawater: equilibrium, kinetics, isotopes, Elsevier Oceanography Series, 65, 2001.

Zhang, H., Blanco-Ameijeiras, S., Hopkinson, B., Bernasconi, S., Mejia, L., Liu, C., and Stoll, H.: An isotope label method for empirical detection of carbonic anhydrase in the calcification pathway of the coccolithophore Emiliania huxleyi, Geochim Cosmochim Ac, 292, 78-93, 10.1016/j.gca.2020.09.008, 2021.

Zhang, H., Torres-Romero, I., Anjewierden, P., Jaggi, M., and Stoll, H.: The DIC carbon isotope evolutions during CO2 bubbling: Implications for ocean acidification laboratory culture, Front Mar Sci, 9, 10.3389/fmars.2022.1045634, 2022.

Ziveri, P., Stoll, H., Probert, I., Klaas, C., Geisen, M., Ganssen, G., and Young, J.: Stable isotope 'vital effects' in coccolith calcite, Earth Planet Sci Lett, 210(1-2), 137-149, 10.1016/S0012-821X(03)00101-8, 2003.

Ziveri, P., de Bernardi, B., Baumann, K., Stoll, H., and Mortyn, P.: Sinking of coccolith carbonate and potential contribution to organic carbon ballasting in the deep ocean, Deep-Sea Res Pt II, 54(5-7), 659-675, 10.1016/j.dsr2.2007.01.006, 2007.

https://doi.org/10.5194/egusphere-2023-2581
Preprint. Discussion started: 9 November 2023

725 Ziveri, P., Thoms, S., Probert, I., Geisen, M., and Langer, G.: A universal carbonate ion effect on stable oxygen isotope ratios in unicellular planktonic calcifying organisms, Biogeosciences, 9(3), 1025-1032, 10.5194/bg-9-1025-2012, 2012.

Tables

Species	Temperature (°C)	Final $CO_{2(aq)}$ (µM)	Culture setup type	$\Delta^{13}C_{c\text{-}DIC}$ (‰ V-PDB ± 1σ)	$\Delta^{18}O_{c\text{-}sw}$ (‰ V-SMOW ± 1σ)	Δ_{47} (‰ I-CDES ± 1SE)
G. oceanica	12	14.66	Batch	-0.40 ± 0.47	32.95 ± 0.34	0.640 ± 0.009
	15	21.56	Continuous	-0.87 ± 1.12	31.29 ± 0.26	0.621 ± 0.009
	15	33.01	Continuous	0.03 ± 0.18	31.57 ± 0.25	0.634 ± 0.008
	15	40.18	Continuous	-0.24 ± 0.13	31.68 ± 0.26	0.637 ± 0.013
	18	6.94	Continuous	-1.15 ± 0.69	31.37 ± 0.13	0.628 ± 0.009
	18	7.95	Continuous	-1.41 ± 0.70	31.03 ± 0.26	0.629 ± 0.005
	18	18.41	Continuous	0.54 ± 1.00	30.65 ± 0.15	0.620 ± 0.004
	18	24.12	Continuous	-0.95 ± 1.00	30.74 ±0.13	0.620 ± 0.010
	18	27.73	Continuous	0.51 ± 1.00	30.63 ± 0.12	0.629 ± 0.008
	18	42.58	Continuous	-0.24 ± 0.35	31.48 ± 0.11	0.633 ± 0.005
	21	5.62	Continuous	-0.24 ± 0.25	30.45 ± 0.14	0.624 ± 0.007
	21	6.18	Continuous	0.75 ± 0.25	30.47 ± 0.17	0.611 ± 0.008
	21	6.18	Continuous	0.69 ± 0.27	30.37 ± 0.22	0.626 ± 0.004
	21	7.63	Continuous	-0.61 ± 0.25	30.44 ± 0.35	0.621 ± 0.005
	21	11.68	Continuous	-0.39 ± 0.15	30.17 ± 0.11	0.618 ± 0.012
	21	12.83	Continuous	-0.43 ± 0.13	30.26 ± 0.07	0.608 ± 0.012
	21	21.23	Continuous	1.22 ± 1.05	30.77 ± 0.33	0.620 ± 0.005
	21	21.23	Continuous	1.22 ± 1.05	30.76 ± 0.33	0.604 ± 0.008
	21	29.48	Continuous	-0.49 ± 0.32	30.74 ± 0.86	0.630 ± 0.007
	21	30.76	Continuous	-0.66 ± 0.32	30.92 ± 0.86	0.625 ± 0.011
	21	43.22	Continuous	-1.21 ± 1.05	30.57 ± 0.34	0.603 ± 0.004
	21	43.22	Continuous	-1.25 ± 1.05	30.56 ± 0.33	0.607 ± 0.006
	21	43.76	Continuous	-0.98 ± 1.05	30.45 ± 0.33	0.611 ± 0.010
	24	13.05	Continuous	0.83 ± 0.34	29.41 ± 0.09	0.599 ± 0.005
	24	13.05	Continuous	0.85 ± 0.34	29.44 ± 0.10	0.598 ± 0.008
	24	13.73	Batch	-0.80 ± 0.28	29.09 ± 0.41	0.605 ± 0.007
	24	14.07	Batch	-0.21 ± 0.28	29.70 ± 0.37	0.611 ± 0.008
	24	16.95	Continuous	0.65 ± 0.34	29.72 ± 0.10	0.607 ± 0.010
	24	19.18	Continuous	-0.87 ± 0.39	29.38 ± 0.14	0.589 ± 0.006
	27	15.11	Continuous	0.61 ± 0.82	29.10 ± 0.13	0.603 ± 0.007
	27	15.11	Continuous	0.61 ± 0.82	29.03 ± 0.11	0.597 ± 0.007
G. muellerae	6	14.40	Batch	-0.88 ± 0.03	33.90 ± 0.28	0.659 ± 0.006
	6	14.57	Batch	-0.57 ± 0.03	34.00 ± 0.28	0.655 ± 0.005
	12	16.34	Batch	0.03 ± 0.21	32.48 ± 0.71	0.648 ± 0.005

https://doi.org/10.5194/egusphere-2023-2581
Preprint. Discussion started: 9 November 2023

	12	21.22	Batch	0.21 ± 0.21	32.98 ± 0.70	0.645 ± 0.008
	18	7.94	Batch	-0.88 ± 0.35	31.28 ± 0.24	0.618 ± 0.010
	18	9.80	Batch	-0.26 ± 0.35	31.31 ± 0.24	0.629 ± 0.009
C. leptoporus	12	17.94	Batch	-2.34 ± 0.42	29.78 ± 0.36	0.645 ± 0.006
	12	17.94	Batch	-2.22 ± 0.42	29.93 ± 0.35	0.652 ± 0.005
	12	19.12	Batch	-2.86 ± 0.49	29.89 ± 0.57	0.636 ± 0.008

Table 1. Overview table for all included data points for Sect. 3, 4.1, 4.2. including temperature (°C), culture setup type, $CO_{2(aq)}$ (µM), $\Delta^{13}C_{c\text{-}DIC}$ (‰; VPDB), $\Delta^{18}O_{c\text{-}sw}$ (‰; VSMOW), and Δ_{47} values (‰; I-CDES). 1 standard deviation (σ) is included for the $\Delta^{13}C_{c\text{-}DIC}$ and $\Delta^{18}O_{c\text{-}sw}$, which take the evolution of the media over time into account, and 1 standard error (SE) for Δ_{47}.

Data type	Slope	Intercept
G. oceanica	0.0377 ± 0.009	0.179 ± 0.104
G. oceanica + *G. muellerae*	0.0360 ± 0.005	0.198 ± 0.063
G. oceanica + *C. leptoporus*	0.0387 ± 0.007	0.168 ± 0.083
Temperature-weighted averages	0.0358 ± 0.006	0.202 ± 0.073
All species	0.0367 ± 0.005	0.190 ± 0.059
Including excluded data	0.0375 ± 0.004	0.181 ± 0.048

Table 2. Slope and intercepts with 1σ for the Δ_{47}-temperature regression using the Williamson-York bivariate least-squares method.

	pH	DIC	$CO_{2(aq)}$
All measured $\Delta\Delta_{47,off}$	0.17	-0.01	-0.09
Continuous setup $\Delta\Delta_{47,off}$	0.27	-0.04	-0.13
Batch setup $\Delta\Delta_{47,off}$	-0.32	0.20	0.11

Table 3. Pearson correlation coefficients (ρ) between $\Delta\Delta_{47,off}$ and pH, DIC, and $CO_{2(aq)}$ for all measurements, continuous culture, and batch culture setup. For all ρ, p-values > 0.05.

	Measured Δ_{47}	Katz et al. (2017)	Peral et al. (2018)	Meinicke et al. (2020)	Anderson et al. (2021)	de Winter et al. (2022)	Daëron and Gray (2023)
$\Delta\Delta_{47,off}$ residuals (ppm ± 1σ)	-0.6 ± 3.4	8.2 ± 2.7	-0.9 ± 2.4	-3.1 ± 1.3	-8.0 ± 1.0	-4.3 ± 1.7	-7.6 ± 0.6
Temperature offset (°C ± 1σ)	0.19 ± 1.12	-2.67 ± 0.88	0.30 ± 0.81	1.04 ± 0.43	2.70 ± 0.32	1.44 ± 0.55	2.55 ± 0.19

Table 4. Average $\Delta\Delta_{47,off}$ residuals relative to our dataset comparing our coccolith calibration equations and those from Katz et al. (2017), Peral et al. (2018), Meinicke et al. (2020), Anderson et al. (2021), de Winter et al. (2022), and Daëron and Gray (2023). Equivalent temperature offset is based on the equivalent Meinicke et al. (2020) Δ_{47} value at the average growth temperature (18.7°C).

https://doi.org/10.5194/egusphere-2023-2581
Preprint. Discussion started: 9 November 2023

740 **Figures**

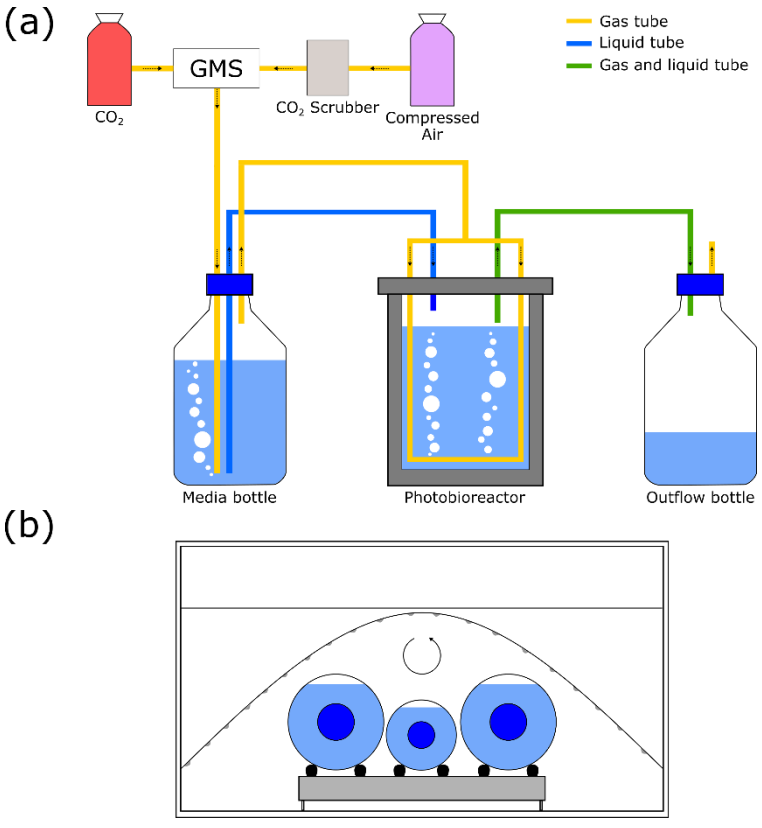

Figure 1. Photobioreactor and incubator systems. (a) Photobioreactor with controlled CO_2 gas input, adjusted from Zhang et al. (2022), (b) Incubator with roller containing 2 2L and 1 1L bottle and LED strip for batch cultures.

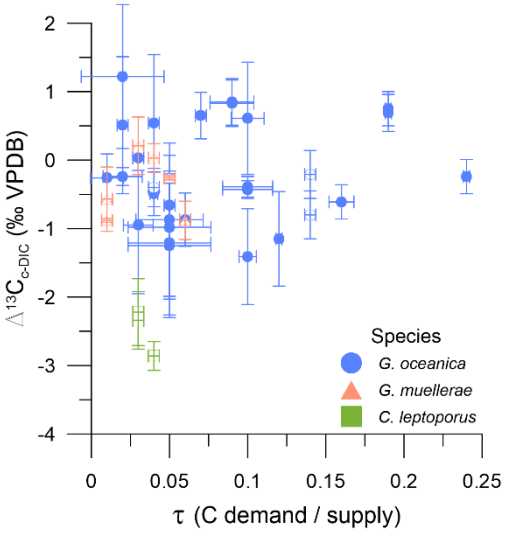

745

https://doi.org/10.5194/egusphere-2023-2581
Preprint. Discussion started: 9 November 2023

Figure 2. Coccolith carbon isotope fractionation relative to external DIC ($\Delta^{13}C_{c\text{-}DIC}$) against the carbon demand vs supply (τ). Blue circles are *G. oceanica*, orange triangles are *G. muellerae*, and green squares are *C. leptoporus*. Open and filled symbols are batch and continuous cultures respectively. Error bars are as described in methods.

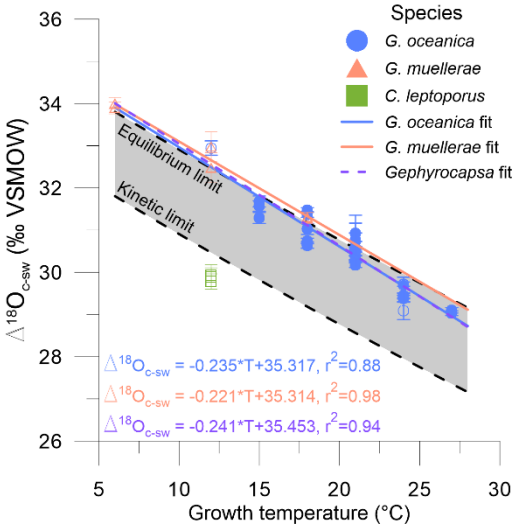

Figure 3. The fractionation of oxygen isotopes in coccolith calcite from seawater ($\Delta^{18}O_{c\text{-}sw}$), both in VSMOW, in relation to the growth temperature in °C. Blue circles are *G. oceanica*, orange triangles are *G. muellerae*, and green squares are *C. leptoporus*. Open and filled symbols are batch and continuous cultures respectively. Linear regression fits are calculated for *G. oceanica* and *G. muellerae* separately, as well as for the whole *Gephyrocapsa* genus, with equivalent formulae. Error bars are as described in methods, temperature error bars are smaller than symbols. The kinetic and equilibrium limits are from Watkins et al. (2014) and defined as $\left(\frac{17747}{T+273.15}\right) - 29.77$ and $\left(\frac{17747}{T+273.15}\right) - 31.77$ respectively.

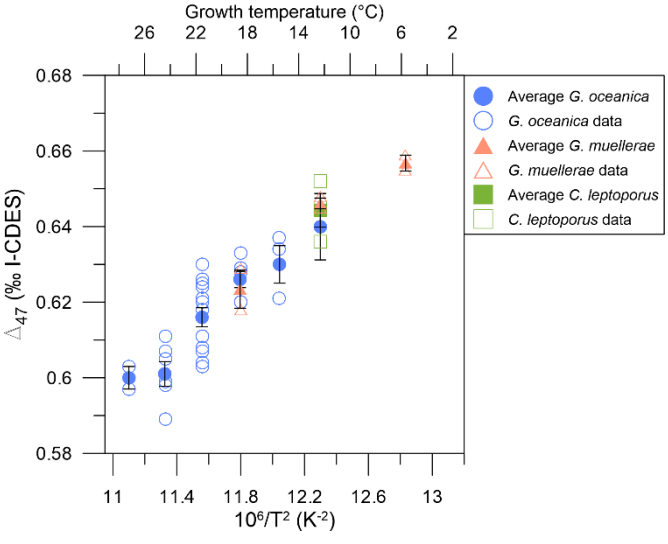

https://doi.org/10.5194/egusphere-2023-2581
Preprint. Discussion started: 9 November 2023

Figure 4. Δ_{47} values from coccolith calcite versus $10^6/T^2$ for all data points and averages. Averages are full symbols, while individual datapoints are empty symbols. Blue circles are *G. oceanica*, orange triangles are *G. muellerae*, and green squares are *C. leptoporus* data. Error bars are as described in methods, temperature error bars are smaller than symbols.

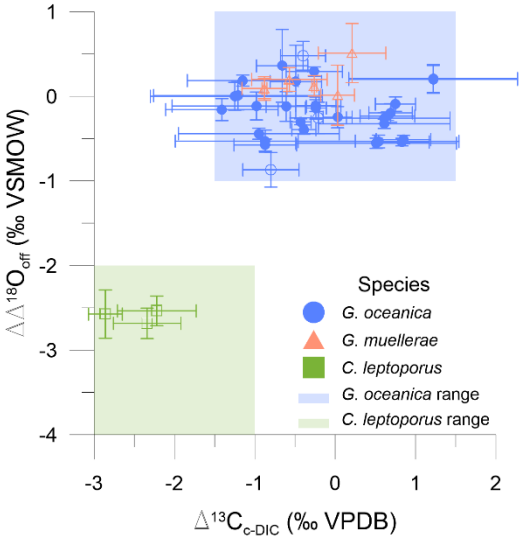

Figure 5. The oxygen isotope offset from the equilibrium limit in Watkins et al., (2014) ($\Delta\Delta^{18}O_{off}$) against the coccolith carbon isotope fractionation relative to external DIC ($\Delta^{13}C_{c\text{-}DIC}$). Blue circles are *G. oceanica*, orange triangles are *G. muellerae*, and green squares are *C. leptoporus* data. Open and filled symbols are batch and continuous cultures respectively. The $\Delta^{13}C_{c\text{-}DIC}$ and $\Delta\Delta^{18}O_{off}$ range of previous *G. oceanica* and *C. leptoporus* studies are given as a blue and green background respectively. Error bars are as described in methods.

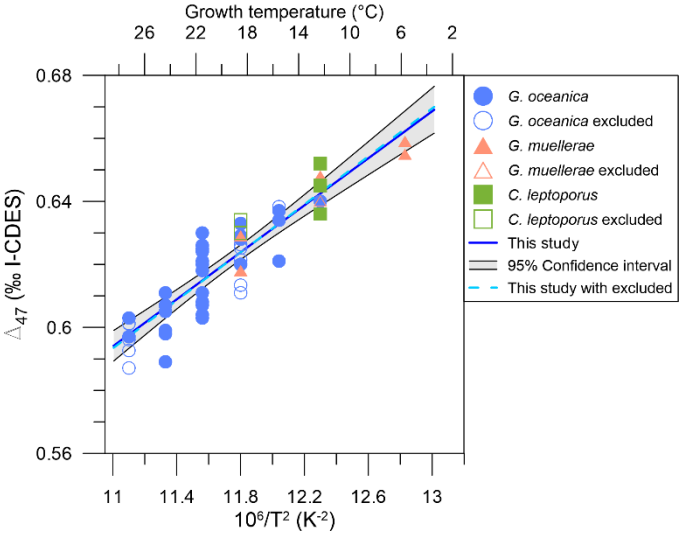

Figure 6. Δ_{47} values compared to temperature (in K) for cultured coccoliths. York regression and its 95% confidence interval are shown as a blue line and light grey envelope. The species are colour and symbol coded following Fig. 2. Blue circles are *G. oceanica*,

https://doi.org/10.5194/egusphere-2023-2581
Preprint. Discussion started: 9 November 2023

orange triangles are *G. muellerae*, and green triangles are *C. leptoporus*. Empty symbols are excluded data but still included for illustration and the coccolith Δ_{47}-temperature calibration.

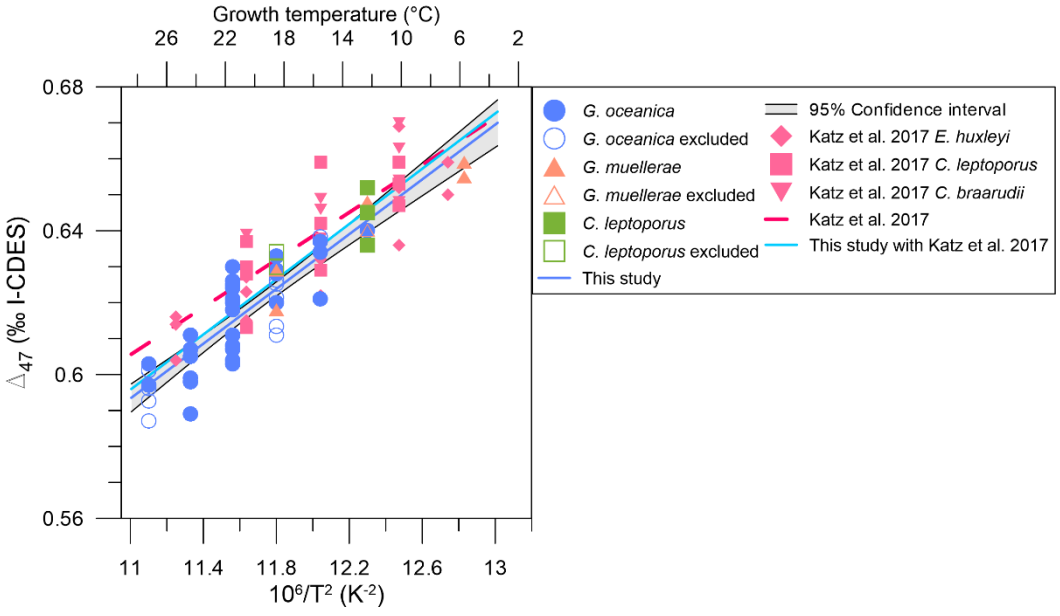

Figure 7. Δ_{47} values compared to temperature (in K) for cultured coccoliths including a previous culturing study by Katz et al. (2017). York regression and its 95% confidence interval are shown as a blue line and light grey envelope. The species and data are colour and symbol coded following Fig. 2. The data from Katz et al. 2017 is in pink. Blue circles are *G. oceanica*, orange triangles are *G. muellerae*, green triangles are *C. leptoporus*, pink diamonds are *E. huxleyi*, pink squares are *C. leptoporus*, and pink cones are *C. braarudii*. Empty symbols are excluded data but still included for illustration and the coccolith Δ_{47}-temperature calibration.

https://doi.org/10.5194/egusphere-2023-2581
Preprint. Discussion started: 9 November 2023

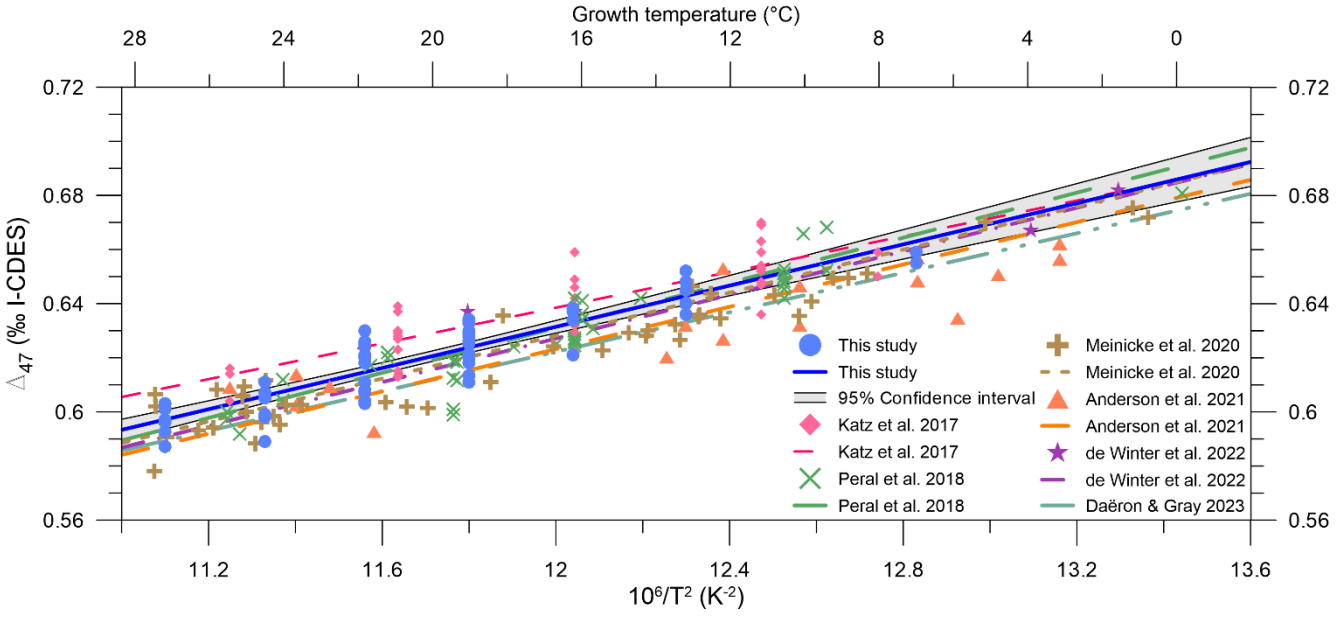

Figure 8. Δ_{47} versus temperature for coccolith calcite and previous biogenic and inorganic calibrations. The York linear fit and 95% confidence interval for the unified coccolith calcite Δ_{47}-temperature is shown as a blue line with grey shading. Katz et al. (2017; pink diamonds), Peral et al. (2018; green X's), Meinicke et al. (2020; brown crosses), Anderson et al. (2021; orange triangles), and de Winter et al. (2022 purple stars). The calibration curves are also shown as dashed lines, with the same colour scheme, Daëron and Gray (2023) is shown as a grey dashed-dot line.

https://doi.org/10.5194/egusphere-2023-2581
Preprint. Discussion started: 9 November 2023

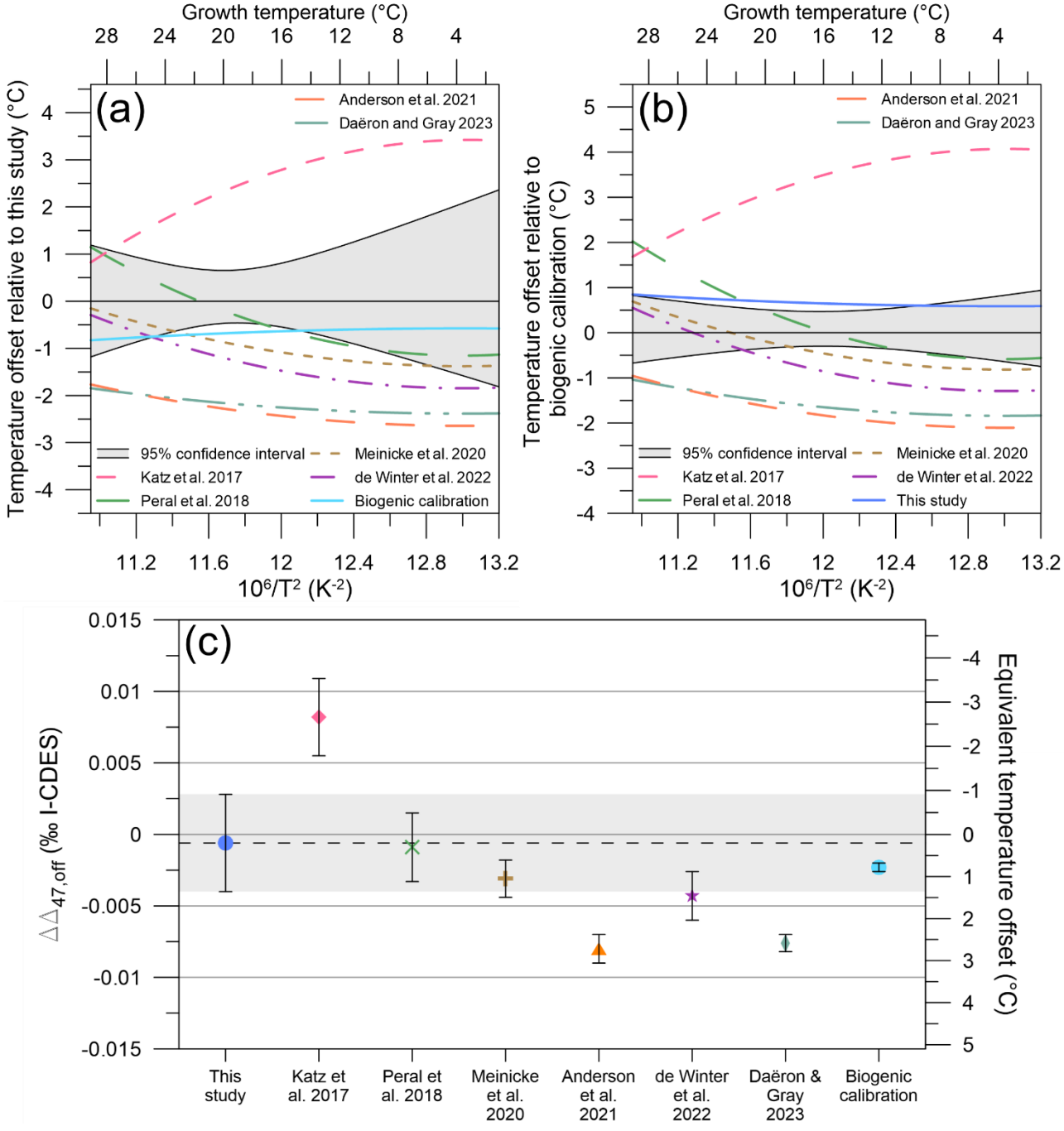

Figure 9. Temperature offset of different Δ_{47}-temperature calibrations relative to (a) our study's equivalent temperature, (b) the general biogenic Δ_{47}-temperature calibration, (c) our study's equivalent at the average growth temperature (18.7°C), with average $\Delta\Delta_{47,off}$ residuals of different Δ_{47}-temperature calibrations relative to this study's dataset. The other studies' calibration data are colour coded following Fig. 8. The general biogenic Δ_{47}-temperature calibration is given as light blue. The 95% confidence interval is given as light grey shading in (a), (b). This study's average $\Delta\Delta_{47,off}$ and range is given as a dotted line and light grey shading in (c).